Document Number**:** H2020-ICT-52/RISE-6G/D4.1

Project Name:
Reconfigurable **I**ntelligent **S**ustainable **E**nvironments for **6G** Wireless Networks
(RISE-6G)

Deliverable D4.1

Deployment and control strategies of RIS based connectivity (Intermediary Specifications)

Date of delivery:	30/04/2022	Version:	1.0
Start date of Project:	01/01/2021	Duration:	36 months

Deliverable D4.1

Deployment and control strategies of RIS based connectivity (Intermediary Specifications)

Project Number:	101017011
Project Name:	**R**econfigurable **I**ntelligent **S**ustainable **E**nvironments for **6G** Wireless Networks

Document Number:	H2020-ICT-52/RISE-6G/D4.1
Document Title:	Deployment and control strategies of RIS based connectivity (Intermediary Specifications)
Editor(s):	Paolo Di Lorenzo (CNIT)
Authors:	Placido Mursia (NEC), Francesco Devoti (NEC), Paolo Di Lorenzo (CNIT), Sergio Barbarossa (CNIT), Marco Di Renzo (CNRS), George C. Alexandropoulos (NKUA), Kyriakos Stylianopoulos (NKUA), Petar Popovski (AAU), Radoslaw Kotaba (AAU), Fabio Saggese (AAU), Emilio Calvanese Strinati (CEA), Fatima Ezzahra Airod (CEA).
Dissemination Level:	PU
Contractual Date of Delivery:	30/04/2022
Security:	Public
Status:	Draft
Version:	1.0
File Name:	RISE-6G_WP4_D4.1_V3.docx

Abstract

This deliverable provides the results of the RISE-6G proposals on architectures, control, signaling, and data flow related to work package 4 “RIS for Enhanced Connectivity and Reliability”, as well as initial performance evaluations of these proposals.

Keywords

Beyond-5G; 6G; RIS; Scenarios; Architectures; Connectivity; Edge computing

Contents

List of Figures

List of Tables

List of Acronyms

5G-NR	5th Generation - New Radio
BER	Bit Error Rate
BS	Base Station
CAPEX	CAPital EXpenditure
CC	Control Channel
CE	Channel Estimation
CSI	Channel State Information
DL	Downlink
DL-DoD	Downlink Direction of Departure
DL-TDoA	Downlink Time Difference of Arrival
DoA	Direction of Arrival
DoD	Direction of Departure
DRL	Deep Reinforcement Learning
E2E	End-to-End
EM	Electromagnetic
EMFE	ElectroMagnetic Field Exposure
ES	Edge Server
GDoP	Geometric Dilution of Precision
KPI	Key-Performance Indicator
LB-AoI	Localisation Boosted - Area of Influence
LoS	Line-of-Sight
LS	Least Squares
MEC	Mobile Edge Computing
MIMO	Multiple Inputs Multiple Outputs
MISO	Multiple Inputs Single Output
MSE	Mean Squared Error
NLoS	Non-Line-of-Sight
NMSE	Normalised Mean Squared Error
NVAA	Non-Value-Added Activities
OFDM	Orthogonal Frequency Division Multiplexing
OPEX	OPerating EXpenditure
PARAFAC	PARAllel FACtor
PL	Physical Layer
RF	Radio Frequency
R-RIS	Reflective RIS
RT-RIS	Reflective-transmission RIS
RIS	Reconfigurable Intelligent Surface
RISC	RIS controller
RISO	RIS Orchestrator
RSSI	Received Signal Strength Indicator
RTT	Round Trip Time
RT-ToF	Round Trip – Time of Flight
Rx	Receiver
SINR	Signal to Interference plus Noise Ratio
SISO	Single Input Single Output
SMSE	Sum Mean Squared Error
SNR	Signal to Noise Ratio
TDoA	Time Difference of Arrival
ToA	Time of Arrival
Tx	Transmitter
UAV	Unmanned Aerial Vehicle
UE	User
UTDoA	Uplink Time Difference of Arrival
UL	Uplink
UL-DoA	Uplink Direction of Arrival
UL-TDoA	Uplink Time Difference of Arrival

1 Introduction

RISE-6G is a 5G-PPP project funded by the European Commission under the H2020 framework. RISE-6G vision hinges on the latest advances on Reconfigurable Intelligent Surfaces (RISs) technology for radio wave propagation control, with the aim of improving this technology, and conceiving sustainable, programmable, and goal-oriented wireless environments. The main objectives of RISE-6G are: (i) the definition of novel architectures and control strategies incorporating multiple RISs; (ii) the study of the fundamental limits of RIS technology based on realistic and validated radio wave propagation models; (iii) the design of algorithmic frameworks enabling high-capacity connectivity, energy efficiency, low EMF exposure, localisation accuracy, and edge computing based on RIS-empowered wireless environments; (iv) prototyping the proposed innovation via two complementary trials with verticals.

Within RISE-6G, work package 4 (WP4) considers the use of RISs for improved wireless connectivity for legacy frequencies and higher-frequency bands. The aim of WP4 is four-fold: (i) Design RISE network architectures and deployment strategies including RIS control signaling for enhanced connectivity; (ii) Establish the fundamentals of communication for RIS-empowered systems; (iii) Design and optimise protocols and methods for RIS control and resource allocation to support high reliability, coverage, low-latency, and high two-way data rate; (iv) Design joint resource allocation and offloading strategies to unlock seamless, reliable, distributed, RIS-empowered edge computing services.

1.1 Deliverable objectives

This document provides the intermediate results related to the first aim of WP4 and covers different KPIs, architectural alternatives, RIS control strategies, as well as data flow and signalling, derived from the various contributions within WP4. One of the main objectives is to determine the best strategies according to the KPIs for an easy and flexible deployment of RISs as the new network elements considering boosted connectivity areas. Two principle operating modes will be considered for the RIS: (1) autonomous, where the RIS is able to sense/decode the radio communication signals and make local decisions; and (2) controlled, where the RIS is controlled by another network element, where there is the possibility for (a) in-band control channel; or (b) out-of-band control. These results serve as input for the work in WP2 on architectures, deployment strategies, and RIS control.

As RISE-6G Project targets very different objectives in WP4, WP5, WP6, the following two-step approach has been chosen, to derive architecture and control signalling requirements.

- During step 1: each WP derives its initial views on requirements on architecture and signalling, based on the WP very specific objectives and the WP's list of technical contributions and innovations; the results of these independent works are reported inD4.1, D5.1 and D6.1, separately.
- During step 2: WP2 uses D4.1, D5.1 and D6.1 as inputs to build a common framework for architecture and control signalling that will be described in D2.5. Therefore, concepts and vocabulary regarding architecture and control signalling may differ in D4.1, D5.1 and D6.1. The name "RIS controller" for instance, may have a slightly different meaning in two different deliverables. However, it will be clearly defined inside each deliverable. Common concepts and terminology which will be defined in D2.5, to be used afterwards during the project.

1.2 Deliverable structure

This document comprises the following sections. In Section 1.3, we provide the basic terminology used along the document and a taxonomy of the RIS, considering aspects related to hardware, control, and operation mode. Section 2 introduces the KPIs that are relevant to the design of RIS control strategies and the deployment of connectivity-enhancing RIS-empowered networks. Section 3 starts with an initial description of the possible architectures for RIS-empowered communications. Then, five architectural

alternatives proposed in RISE-6G are detailed, considering different scenarios involving static and nomadic integration of RISs in wireless networks, and RIS-empowered mobile edge computing. Section 4 tackles RIS control methods and signaling, considering specifically channel estimation, allocation of transmission resources, and adaptation of the transmission parameters. This section details seven RIS control approaches, which determine the RIS configurations needed for supporting RIS-enhanced communication. In Section 5, we describe the provide the data flow and signaling, and time diagrams for selected architectural and control alternatives given in Section and Section 4. Finally, Section 6 concludes the deliverable with recommendations for the overall RISE-6G architecture.

1.3 Definitions and taxonomy

RIS is a new network element and its integration into the network infrastructure requires a structured approach that defines both the roles of the RIS as well as the protocols between the RIS and the rest of the system [ACP22], [CAS21], [CAW21]. The RIS phase configuration controls the wireless channel over which communication takes place, and thereby an explicit control of the RIS configuration must be performed to optimise the specific performance metric. The architecture must consider that the RIS is envisioned as a multi-purpose element, used for communication, sensing, and positioning. The required architecture is envisioned to include the following components:

- **RIS:** is the reflect-array or meta-material that is directly controlled by an associated RISC. The expected time granularity of RIS reconfiguration is between 100 microseconds and 10 ms. Advanced configuration may make the RIS (logically) connected to a CU/DU of the 3GPP RAN architecture.
- **RIS controller:** the controller associated to a RIS device and located at that device. It is responsible for switching the configurations (states of the RIS elements). RISC may differ in terms of complexity and capabilities; it may receive orders from someone else, in which case it simply acts as an interface that configures the RIS elements based on external explicit instructions (Controlled RIS) or operate on its own (Autonomous RIS). In the former, the controller may directly interact with a RAN element(s). Expected time granularity: 10-50 ms.
- **RIS orchestrator:** the orchestrator is placed on a higher (hierarchical) layer and orchestrate multiple RISCs and/or RAN elements. It can directly interact with the 3GPP AMF and ETSI MEC orchestrators, or the ETSI NFV orchestrator. Time granularity is expected between 100 ms and a few seconds.

The term RIS comprises many different hardware with different capabilities. Here, we briefly define the taxonomy of the RIS. In Table 1, we present the different hardware for the RIS [JAB22], depending on the capability of operation; Table 2 presents the differences of the control channel used to control the RIS operation; Table 3 provides the definition and differences between autonomous and controlled RIS.

Table 1: Hardware taxonomy

Hardware category	General definition	Capabilities
nearly-passive	No RF chains, only ultra-low-power elements to change the reflection states.	Changing the reflection state of its elements.
quasi-active	Includes up to N receiving RF chains, where N is the number of tunable elements.	Changing the reflection state of its elements; can collect measurements in baseband for performing sensing/parameters estimation (in time orthogonal manner with reflection or simultaneously); can also have processing capabilities to perform localisation, channel estimation, etc.
active	Includes transmitting RF chains, where N is the number of tunable elements.	Changing the reflection state of its elements; can also perform reflection amplification or transmit their own signals.

Table 2: Control channel taxonomy

Implicit CC		There is no dedicated CC or signals over which explicit instructions are sent to the RISC. As such, all decisions wrt. RIS operation must be made locally by the RISC. However, these decisions can be based on other received and interpreted signals (e.g. pilot symbols, UE-scheduling information), hence they implicitly (indirectly) control RIS's behavior.
Explicit CC	Out-of-band	The RISC communicates with the RIS using resources that are orthogonal to the RIS operational spectrum resources; control DOES NOT influence the operation of the RIS (simpler CC design, possibly lower spectral efficiency).
	In-band	Control employs resources overlapping the RIS operational spectrum resources; control DOES influence the operation of the RIS (more complex CC design, possibly higher spectral efficiency).

Table 3: Operation mode taxonomy

Controlled RIS	**Autonomous RIS**
The RIS operations are controlled by an external entity providing the main computational processing, and informing the RISC through the explicit CC.	The RIS operations are defined by the RISC on its own, without involving external entities. An explicit CC may be present for communicating synchronization or feedback information.

2 Metrics and KPIs

2.1 KPIs for communication channels

This section introduces the KPIs that are relevant to the design of RIS control strategies and the deployment of connectivity-enhancing RIS-empowered networks. There is a close correspondence with what is described in Deliverables D2.2 and D2.4 of this project which concern the general KPI definitions. However, this document includes a more detailed description of the metrics specifically relevant to WP 4, while introducing novel specifications for control signalling.

The metrics presented below constitute ubiquitous performance indicators in wireless communications, which, in most cases, have been redefined or extended to account for the introduction of the RIS in the communication system. At the same time, special highlight is given to the KPIs introduced to accommodate specific contributions of this deliverable (namely, for control signalling and MEC operations).

2.1.1 Latency

In a communications system, ***latency*** expresses the time delay between the initiation of an event and the perception of its effect. It is one of the key performance metrics in current and next-generation communications. Indeed, 6G specifications target end-to-end (E2E) latency objective of up to 10μs [GRT21]. From a wireless system engineering perspective, we consider the Physical Layer (PL) latency, which is given by the sum of the following components [XH21]:

$$T_{PL} = T_{que} + T_{ttt} + T_{proc} + T_{prop} + T_{retr}$$

where

- T_{que} is the queueing latency arising from the waiting time of the current packet until the transmission of the previous packet is completed.
- T_{ttt} (time-to-transmission) is the time needed for the packet to be forwarded to the physical link.

- T_{proc} denotes the processing latency which accounts for the operations applied to the transmitted data (e.g., encoding/decoding, precoding/combining, modulation/demodulation, channel interleaving and estimation, scrambling, data and control multiplexing).
- T_{prop} expresses the propagation time of the electromagnetic waves through the channel.
- T_{retr} captures the delay induced by retransmissions in case of packet loss when low-reliability links are involved.

In the context of RIS-based connectivity, the T_{proc} component is of particular interest since it is directly affected by the deployment and control strategies adopted.

Furthermore, depending on the system under examination, specific sub-components of the processing latency can be defined. In the sequel, we also highlight the E2E latency in the MEC context, which depends on the nature of the computation offloading.

Static computation offloading

Static computation offloading deals with brief time applications, where mobile users send a single computation request, typically also specifying a service time. Let $A_k(t)$ be the number of input bits required by the application run by user k at time t, and let $w_k(t)$ be the number of Central Processing Unit (CPU) cycles associated with the computing task. Then, the overall E2E delay of UE k is composed of three terms: (i) an UL communication time $\Delta_k^u(t)$, needed by the device to send the input bits to the BS; (ii) a computation time $\Delta_k^c(t)$, needed by the Edge Server (ES) to process the input bits and run the specific application; (iii) a DL communication time $\Delta_k^d(t)$, needed by the BS to send the result of computation back to the UE(s). In summary, the overall E2E latency at time t is given by:

$$\Delta_k\,(t) = \Delta_k^u(t) + \Delta_k^c(t) + \Delta_k^d(t) = \frac{A_k(t)}{R_k(t)} + \frac{w_k(t)}{f_k(t)} + \frac{B_k(t)}{R_k^d(t)}$$

where $R_k(t)$ is the uplink rate from UE k to the BS, $f_k(t)$ is the CPU frequency allocated by the edge server to UE k, $R_k^d(t)$ is the downlink rate from the BS to UE k, and $B_k(t)$ is the number of output bits of the application run by the ES on behalf of UE k. In static computation offloading, communication and computation resources are orchestrated to guarantee that the overall E2E delay $\Delta_k\,(t)$ is less than or equal to an application-dependent requirement, say L_k for all t.

Dynamic computation offloading

In *dynamic computation offloading*, each device continuously generates data $A_k(t)$ to be processed rate (e.g., the transmission of a video recorded by a UE to be processed by the ES for pattern recognition or anomaly detection). Then, a queueing system is used to model and control the dynamic data generation, transmission, and processing. At each time slot t, each user buffers data in a local queue $Q_k^l(t)$ and transmits them to the AP at the transmission rate $R_k(t)$. The local queue update follows the rule:

$$\boldsymbol{Q_k^l(t+1) = max\left(0, Q_k^l(t) - \tau R_k(t)\right) + A_k(t)}$$

where τ is the duration of the time-slot used for scheduling the resources.

Then, the BS receives data from each device k and sends the data to the ES, which processes J_k bits-per-cycle, where J_k is a parameter that depends on the application offloaded by device k. Thus, the computation queue at the ES evolves as:

$$\boldsymbol{Q_k^c(t+1) = \max(0, Q_k^c(t) - \tau f_k(t) J_k\,) + \min\,(Q_k^l(t), \tau R_k(t))}$$

Finally, the BS sends back to each user the bits resulting from the computation, draining a downlink communication queue that evolves as:

$$\boldsymbol{Q_k^d(t+1) = \max\left(0, Q_k^d(t) - \tau R_k^d(t)\,\right) + c_k \min\,(Q_k^c(t), \tau f_k(t) J_k)}$$

where c_k denotes the ratio between output and input bits of the application required by user k. Thus, the E2E delay experienced by offloaded data is related to the sum of the three queues

$$\boldsymbol{Q_k^{tot}(t) = Q_k^l(t) + Q_k^c(t) + Q_k^d(t).}$$

From Little's law, given a data arrival rate $\bar{A}_k = \mathbb{E}[A_k(t)]$, (where $\mathbb{E}[.]$ is the expectation) the average latency experienced by a new data unit from its generation to its computation at the ES is:

$$\boldsymbol{\bar{D}_k = \lim_{T\to\infty} \frac{1}{T}\sum_{t=1}^{T} \mathbb{E}\left[\frac{Q_k^{tot}(t)}{\bar{A}_k}\right].}$$

Thus, in this dynamic context, an average E2E delay constraint can be written as:

$$\boldsymbol{\lim_{T\to\infty} \frac{1}{T}\sum_{t=1}^{T} \mathbb{E}[Q_k^{tot}(t)] \leq Q_k^{avg} = D_k^{avg}\bar{A}_k}$$

More sophisticated probabilistic constraints can also be imposed on the maximum tolerable delay.

2.1.2 Spectral efficiency and throughput

In this sub-section, we provide an example of definition of the ***spectral efficiency (SE)*** metric, which concerns the rate of reliably transmitted information over the allocated communication bandwidth B. The central concept behind spectral efficiency is the (received) Signal to Noise Ratio (SNR) which expresses the ratio between the power of the transmitted signal as it reaches the UE, over the power of the background noise. The presence of the RIS affects the received power of the end-to-end channel by reflecting the impinging EM waves so that they form beams of concentrated power to desired locations. For multi-user communications, this idea extends to the Signal to Interference plus Noise Ratio (SINR), which also captures the interference signals appearing due to the simultaneous communication of multiple ends.
Formally, the achievable SE with respect to a UE depends on the UE's SINR. For instance, the achievable SE with respect to a UE k is given by

$$\boldsymbol{\mathrm{SE}_k = \log_2(1 + \mathrm{SINR}_k) \quad (\mathrm{bits/s/Hz})}$$

and the *sum-rate over the allocated bandwidth* (i.e., the sum of individual rates for all UEs) reads as:

$$\boldsymbol{\mathcal{R} = \sum_k \mathrm{SE}_k}$$

Finally, the throughput of the considered system is finally given by $\boldsymbol{T = B\mathcal{R}}$.

2.1.3 Reliability

We define the notion of ***reliability*** of the communication by considering a given minimum SINR threshold denoted as θ, which is necessary to decode the incoming signal. We define the set of UEs whose received SINR is greater than θ as

$$\boldsymbol{\mathcal{U} = \{k : \mathrm{SINR}_k \geq \theta\}}$$

RIS-Enabled systems are expected to enlarge the network area in which the received SINR of a given UE is above a given threshold, and thus sufficient for successful decoding of the incoming signal.

2.1.4 Bit Error Rate and Bit Error Ratio

Considering a digital transmission, the bit error rate defines the number of bits received incorrectly by the end node per unit time. The normalized version of this metric, the ***Bit Error Ratio*** (BER) concerns the number of incorrect bits as a proportion of the total number of bits transmitted.

2.1.5 Energy efficiency

The ***Energy Efficiency*** (EE) for a downlink communication from a BS to a UE is defined as follows:

$$\boldsymbol{EE = \mathcal{R}/\mathrm{P}\ (\mathrm{bits/s/Hz/Watt})}$$

where $\boldsymbol{\mathcal{R}}$ is the sum data spectral efficiency and P is the total power consumption.

2.1.6 Channel estimation accuracy

For the specific problem of channel estimation, we consider the ***Normalized Mean Squared Error*** (NMSE) to assess the performance of the estimation process. Specifically, NMSE (in dB) is defined as:

$$\mathbf{NMSE} = \mathbb{E}\left[10\log_{10}\frac{\left\|\mathbf{H}-\widehat{\mathbf{H}}\right\|_F^2}{\|\mathbf{H}\|_F^2}\right]$$

where $\mathbf{H}$ and $\widehat{\mathbf{H}}$ are the true and estimated channel matrices, respectively, and $\|\cdot\|_F$ is the Frobenius norm.

2.2 KPIs for control channels

The design of the control channel of the RIS can affect the performance of the communication system. To that end, it is important to define relevant performance indicators assessing the efficiency of the investigated control methodologies both as standalone components, as well as integrated parts of the envisioned deployment strategies.

Depending on the type of the CC, different computational resources are employed by the control mechanism that may consume part of the available bandwidth or transmission frame (a detailed explanation of the control strategies is given in section 4). As a result, the KPIs presented in the previous section can be exploited to evaluate the overall performance of a system with integrated control strategies, by considering only the resources allocated to the data transmission part of the system (rather than to the control signals).

2.2.1 Control Latency

Extending the definition of section 2.1.1, we define the ***control latency*** T_{contr} as the time delay from the time instant when the configuration of the RIS (or a change from a previous configuration) is specified, to the instant after the surface has changed its phase-shifting state. It can be expressed as:

$$T_{contr} = T_{PL}^{contr} + T_{conf}$$

where:

- T_{PL}^{contr} denotes the physical layer latency, as described in section 2.1.1, here concerning only the control signal. The nature of this delay depends heavily on the type of control channel and RIS method of operation. When wired out-of-band control infrastructure is available, (i) the processing delays are smaller, (ii) T_{prop} concerns the propagation of the information bearing (typically electronic) signal, and (iii) there are hardly retransmissions due to the increased reliability of the medium. For out-of-band and in-band control channels, this delay is identical to the latency experienced by the data stream. When considering autonomous RISs this term can be ignored.
- T_{conf} expresses the configuration adaptability of the surface, i.e., the time delay needed for the surface to update the states of its elements. On one part, this delay depends on the computation capacity of the RISC. More importantly, the architecture and manufacturing of the surface affect the state-transition intervals of the individual elements. The quantification of this behavior requires more investigation since it depends on the integrated meta-material elements, and it falls therefore under the objective of Work Package 3 of this project. As previously mentioned, the expected time granularity is 10-50 ms. Nevertheless, it is worth mentioning that it is conceivable for delays to be introduced when changing the complete configuration (i.e., the state of all the elements) of large surfaces.

Let it be noted that the definition of the control latency does not include any of the delays incurring from the algorithmic part of the configuration selection nor the time needed for its execution. The algorithmic considerations are discussed per case in the relevant sections of the control strategies and algorithmic requirements. The exact execution-time delays depend on the software and hardware selected for the system implementation, which falls out of the scope of this deliverable.

2.2.2 Control Reliability

The reliability of the control signals can be measured with the aforementioned BER and reliability KPIs of the previous section. Note that, in both cases, the receiving end of this case is the RIS, instead of the intended UEs. Therefore, it is likely that the KPI values for the control signals differ substantially from the KPI values of the E2E communication. Ultra-high control reliability is a principal objective in the deployment of RIS based solutions.

2.3 KPIs for quasi-active and active RISs

For RIS hardware architectures with receive- and transmit-RF-chains [AAS21], [ASA21], [JAB22], [AV20], [TKB22] special KPIs are introduced to reflect the multiple objectives of the surfaces. Those depend on the exact operation and/or application of the RIS, namely:

- The NMSE metric can be defined for sensing RISs that perform parameter or channel estimation.
- For surfaces capable of performing reflection and amplification, the communication performance metrics of section 2.1 can be applied.
- When considering surfaces that transmit their own information (to facilitate improved control algorithms), once again, the same KPIs are to be applied for evaluation. In this case, only the communication link between the RIS and the network's computational infrastructure is to be taken into consideration, rather than the E2E communication system.

3 Architectures and strategies

3.1 Deployment strategies

The first problem to be addressed when designing architectures and strategies of any new network element is its deployment in the environment. Indeed, the location of the RISs determines how they should be physically interconnected with the rest of the network and what is their optimal configuration at a given time instant. RISs require ad-hoc design, deployment, and management operations to be fully exploited. Indeed, while RISs properly steer the reflect beams towards specific directions, interference is also focused onto unwanted areas, if not properly manipulated. This issue exacerbates the overall deployment complexity calling for advanced optimisation techniques to strike the optimal trade-off between RISs density and the corresponding spurious detrimental interference.

In the literature, the BSs deployment problem has been exhaustively investigated. However, existing works are based on the isotropic antenna radiation assumption making the problem easy-to-solve via graph-coloring algorithms or convex programming approaches. When dealing with directive transmissions — e.g., mmWaves above 6 GHz — a new degree of freedom is introduced: the beam orientation. Specifically, BSs operating at mmWaves must be properly placed and electronically oriented to effectively point the radiated beam towards specific locations leveraging on the available CSI. Nonetheless, an ideal RISs deployment is harder to achieve. On the one hand, the optimal RISs deployment requires a priori information on the applied RISs configurations; on the other hand, the optimal RISs configurations can be obtained only upon fixing the BSs and RISs positions. To overcome this issue and make the analysis tractable, simplistic assumptions on agnostic RISs optimisation can be done [MFC21]. However, a full exploitation of the RISs capability to improve network performance requires advanced modelling and optimization, as detailed below.

3.1.1 Boosted communication and enhanced coverage

The deployment problem is tightly coupled with the RIS application scenario. In the context of indoor scenarios, RISs are considered as the best candidate to solve the mobile dead-zone problem by enabling very-dense RIS-based network deployment at low CAPEX. For instance, in Figure , we illustrate an existing network infrastructure in a real railway station, which however may fail to guarantee satisfactory performance within the entire environment. In such circumstances, ad-hoc RIS design and deployment strategies might be the correct answer to solve the dead-zone problem with a limited investment. It is

important to highlight that active beamforming via an antenna array at the transmitter side and passive beamforming in the channel via RIS can complement each other and provide even larger gains when they both are jointly optimised. In this regard, the choice of an objective function is of paramount importance, especially for massive access scenarios. Indeed, successful RIS deployments require agile and low-complexity algorithms to be run *online* at the RISC.

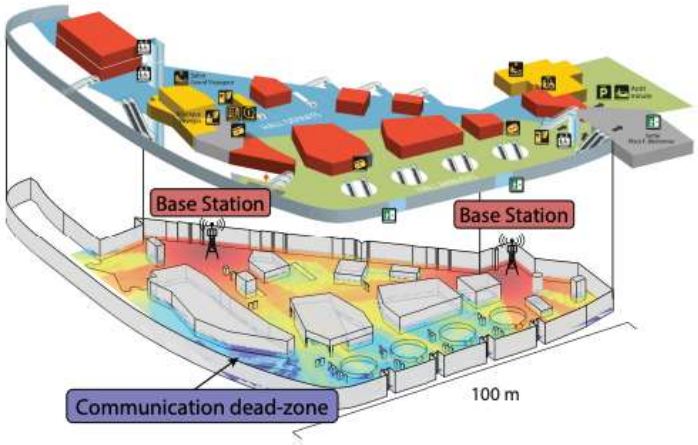

Figure 3-1: Indoor RIS deployment scenario.

3.1.2 Static versus Nomadic

RISs can be integrated in the wireless networks in two different ways, namely: *i) static* RIS, i.e., by mounting them on the facade of buildings to assist in the communication to/from the UEs; and *ii) nomadic* RIS, i.e., by mounting them on-board moving objects such as UAVs, HAP, FWA, or even cars/public transport. While the former category is well understood and developed in the literature, little is known about the latter category, which still requires to be explored. UAVs have attracted considerable interest owing to their agile deployments and the ability to establish a LoS link towards ground users thereby acting as flying access points avoiding obstacles that impair the overall communication quality [MSB18]. Such solutions, namely air-to-ground networks are proposed to bring back-up connectivity in natural disaster areas and/or leverage on advanced sensing and localisation techniques exploiting the cellular protocol stack to find missing people as depicted in Figure 3-2: UAV equipped with a lightweight RIS in an emergency scenario. [ASC21].

In this context, RISs may be mounted as substitutes to bulky active components such as conventional BSs on board the flying device [PSZ21]. By allowing the UAV to carry an inherently light-weight and passive device on board such as an RIS, nearly all the available power can be devoted to enlarging the range of operation, while simultaneously achieving highly selective beamforming [AJH20].

Figure 3-2: UAV equipped with a lightweight RIS in an emergency scenario.

A widely adopted assumption in the SoA control architectures is to consider the RIS-bearing platform as in a predefined location in space with negligible orientation and position variations during the communication phase, while its position is updated only within the displacement phase. However, such assumption does not hold in nomadic RIS scenarios, wherein the platform maneuvering, and several atmospheric phenomena can change its position and orientation even during the communication operations, leading SoA solutions to be potentially inefficient — or even unfeasible — to operate in realistic conditions. For the case of UAVs, as they are hovering at a certain altitude, their motion is influenced by a deterministic component, which is due to the *intentional* maneuvering of the UAV, i.e., following a predefined trajectory, and a *random* component, due to unpredictable factors such as atmospheric conditions including wind, rain, and humidity, imprecise maneuvering, non-ideal UAV instrumentation, etc. Such movements result in translations and rotations of the surface of the on-board RIS, which in turn lead to misalignment of the transmit and reflected beams. This effect is further exacerbated by the highly directive nature of mmWaves beamforming at the RIS and can ultimately result in loss of connectivity at the user-side. Moreover, the rapid variability of the meteorological phenomena and their difficult predictability in the short-term, make real-time RIS control unpractical to overcome the UAV undesired movements effect.

3.1.3 Edge computing

With the advent of beyond 5G networks, mobile communication systems are evolving from a pure communication framework to enablers of a plethora of new services (including verticals), such as Industry 4.0, Internet of Things (IoT), and autonomous driving, building on the tight integration of communication, computation, caching, and control [NTH19], [MDB21]. In this context, a prominent role will be played by Mobile Edge Computing (MEC), whose aim is to move cloud functionalities (e.g., computing and storage resources) at the edge of the wireless network to avoid the relatively long and highly variable delays necessary to reach centralised clouds [BSD14]. MEC-enabled networks allow UEs to offload computational tasks to nearby processing units or Edge Servers (ESs), typically placed close to Access Points (APs), in order to run the computation on the UEs' behalf. However, moving toward mmWave communications (and beyond), poor channel conditions due to mobility, dynamicity of the environment, and blocking events, might severely hinder the performance of MEC systems. In this context, a strong performance boost can be achieved empowering MEC with RISs, with the aim of increasing uplink and downlink capacities, and to counteract channel blocking effects in the case of directive mmWave communications [DMC21]. In such a dynamic context, the available resources (i.e., radio, RISs, computation, etc.) must be properly managed to provide the UEs with a satisfactory Quality of Service. Since the E2E delay includes a communication time and a computation time (cf. Sec. 2.1.1), the edge resources must be managed jointly, learning over time the best joint resource allocation in a dynamic and data-driven fashion. In this architecture, the ES has the primary role of computing resource, but also represents the central unit that performs online resource optimisation and RIS control.

3.1.4 Control and monitoring of EMFE radiation

Recently, there has been growing interest in the EMFE utility metric, as defined in Deliverable D2.4, Section 2.10 and Deliverable D6.1, Section 3.1. Such metric accounts for the electromagnetic field exposure received by a non-intended UE in the system or the (self) exposure produced by a given UE. As described in Section 3.2.1 of Deliverable D6.1, RIS-aided EMF-Aware beamforming schemes are proposed with the objectives of delivering downlink data from the BS to the UE with maximum received power at the target UE, whilst complying with the EMFE regulation, thus optimising the considered EMEFE utility metric [APV21][APV221][APV222]. The minimum architecture requirements are depicted in Figure3-3 in Section 3.2.1 of Deliverable D6.1.

3.2 RIS Control Plane

Control architectures for RIS-aided networks can be divided into two separate layers: network-side control and RIS platform control. The former is physically located in the conventional cellular network, and consists of a processing unit that, given a set of policies and Quality of Service requirements, jointly optimises the active beamforming at the BS and/or at the receiver-side, and the passive beamforming at

the RIS if there exists an (explicit) CC.[1] Moreover, it deals with acquiring CSI and extracting the associated relevant channel parameters, and managing the RIS handover procedure in the case of nomadic RIS. On the other side, the RIS platform control is given essentially by the RISC and specific device platform control in the case of nomadic RISs, which oversees maneuvering of the RIS-bearing platform. The RISC is physically located at the RIS and triggers RIS settings (i.e., predefined phase shifts) and may deal with its optimisation in the case of autonomous RIS (implicit CC, see below). As described above, to get out of nomadic-RIS networks in a practical scenario, the mitigation of mobility effects caused by the movement of the RIS-bearing platform, which can be predefined (e.g., maneuvering) or unwanted (e.g., perturbations), is a key point. It is thus essential to design enhanced control architectures enabling a transmission optimisation tightly coupled with the device mobility pattern. As described in Table 2, the CC of RIS-aided networks can be either *i)* implicit or *ii)* explicit. In the former case, the RISC optimises the configuration based on local information and does not communicate with the network, whereas in the latter case the RISC communicates with the rest of the network.

3.2.1 RIS-aided neworks with controlled RIS (explicit CC)

When aiming at maximising the sum rate of RIS-aided networks it is essential to design enhanced control architectures enabling a transmission optimisation tightly coupled with the current CSI, which includes both UE and RIS mobility pattern (if any). Since the RIS is typically conceived as a lightweight easy-to-deploy device, the data processing related to any optimisation task is carried out at an external entity, e.g., the BS-side controller, which is part of the traditional mobile communication network. Such a unit is in charge of detecting active UEs and collecting the associated channel measurements. The relevant CSI must be generated at a rate that must be adapted to the local mobility pattern of both UEs and RISs. Real-time maneuvering instructions and RIS sensors' output may also be incorporated in the communication optimisation process, if available.

The optimised RIS configuration, both for CSI acquisition/activity detection or communication purposes, is sent-out by the network to the RIS controller via the available CC, dubbed as explicit CC. Moreover, in the case of nomadic RIS, the network-side controller informs the RISC of its BS association. An anticipated drawback of such a solution is the use of precious time/frequency resources to be devoted to the CC. In particular, the (explicit) CC can be either in or out-of-band. In the former case, the control messages employ overlapping resources with the communication phase. Such a solution requires a complex CC design but allows for limiting the amount of communication overhead. In the latter case, the control messages are allocated in orthogonal resources as compared to the communication phase, leading to greater overhead, which limits the achievable throughput. On the other hand, such a solution allows for a simpler CC design.

3.2.2 RIS-aided networks with autonomous RIS (implicit CC)

In the case of implicit CC, the RIS controller optimises the RIS based only on local CSI. The lack of communication with the network separates the RIS configuration problem from the optimisation of the BS beamforming, which are tightly coupled with the explicit CC. It is worth pointing out that without a CC between the network and the RISC the presence of the RIS is transparent to the rest of the network from the control point of view. Indeed, once the RIS is configured, the BS can detect additional, potentially enhanced, multipath components provided by the RIS through standard channel sounding operations and exploit their availability with a proper beamforming optimisation. Therefore, implicit control strategies facilitate agile deployment and configuration of the RIS devices, which are essential features to easily integrate the RIS technology into existing networks and standards and expedite the penetration of the RIS devices in the market. As a side-effect, the RIS hardware needs to have the capability to process the incoming signal to acquire local CSI, therefore either quasi-active or active RIS hardware is necessary.

3.3 Contributions from RISE-6G

The main architectural characteristics of the RISE-6G contributions are listed below in Table 4.

[1] Note that the network-side controller is represented by the conventional node that is typically in charge of the BS and/or receiver configurations and collecting CSI in SoA RAN architectures.

Table 4: Main architectural characteristics: Contributions from RISE-6G

Architecture	A-0: RIS-Aware Indoor Network Planning.	A-1: RIS-Enabled Beamforming for IoT Massive Access.	A-2: RIS-Empowered UAV Communications for Robust and Reliable Air-to-Ground Networks.	A-3: A Self-Configuring RIS Solution Towards 6G.	A-4: RIS-empowered Mobile Edge Computing
# BS	multiple	1	1	1	1
# RIS	multiple	1	1	1	Multiple/Single
# UEs	1	Multiple	Multiple	Multiple	Multiple
UE mobility	Static	Static	Static	Static	Static/slow mobility
RIS mobility	Static	Static	Mobile	Static	Static
Frequency band	Any	Any	Any	Any	Any/High frequency bands
LoS/NLoS	LoS	Both	LoS	LoS	Both
KPI	Max min SNR	SMSE	Max min SNR	Sum-Rate	Energy, Latency

3.3.1 Contribution #A-0: RIS-Aware Indoor Network Planning

Motivation and context

We consider a realistic RIS-enabled wireless scenario where a total of *N* multi-antenna *nearly-passive* RISs may be applied as to obtain enhanced coverage areas and solve the so-called "communication dead-zones". The given target area of interest is served by *M* multi-antenna BSs exclusively through the RISs due to blockage or shadowing. Furthermore, we assume that the location of the BSs is fixed and that each RIS is used and controlled by a single BS via a separate (wired or wireless) control link. The considered scenario is depicted in Figure .

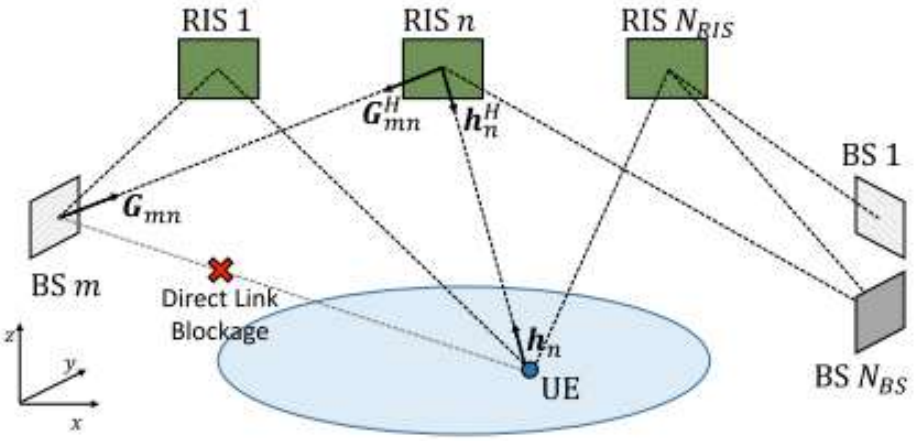

Figure 3-3: Geometrical representation of the considered planning scenario.

In [AES22] we present RISA, a RIS-Aware network planning solution that iteratively triggers RISs configurations and optimally places the required number of RISs within a given target area, without any unpractical assumption on available CSI. Our objective is to jointly optimise the active transmit beamformers at the BSs as well as the RISs placement, their passive beamforming configurations, and their controlling BSs, which in turn dictate the optimal end-to-end BS-UE associations. The resulting optimisation problem is highly non-convex and extremely difficult to tackle due to the intricate coupling between the BSs-RISs and BSs-UE associations, and the joint active-passive beamforming configurations throughout the network. Therefore, for the sake of analytical tractability, we only consider one-RIS path

and a cellular-like architecture in which each RIS provides coverage to one contiguous subarea, thus reducing the scope of the interference generated by the remaining RISs to the sole overlapping area edges. We would like to highlight that at planning stage, the RISs beamforming design for area coverage enhancement cannot take advantage of the knowledge of the instantaneous CSI of any UE in the area. Hence, although RISs controlled by the same BS can be configured to cover the same subarea, it is highly complex to enforce in-phase constructive interference of signals incoming from different RISs even if transmitted by the same BS.

Methodology

For the sake of analytical tractability, we assume that the RISs are deployed only at specific locations, namely candidate sites (CSs) to reflect the fact that network operators are required to meet logistical, administrative, and physical constraints in real-life scenarios. Nonetheless, in the absence of CSs, our multi-RIS planning may be likewise executed by considering any sampling of the deployment area. Besides, we sample the target area by means of T test points, which represent the possible locations of the *typical UE*. Our planning solution outputs the set of the RISs to be deployed while providing the optimal BS-RIS-UE association at each test point. We thus formulate the problem of maximising the worst SNR among all possible locations of the *typical UE* within the target area. However, such problem is nonconvex and highly complex to tackle. Therefore, we decouple the RISs and BSs beamforming configurations from the planning problem itself by configuring each RIS to provide coverage to one contiguous subarea, assuming that each BS radiates all its available power towards each of its associated RISs in a time-division multiple access (TDMA) fashion. Given sufficient coverage in the area, multiple users in each subarea can be separated by conventional multiple access techniques, such as TDMA or orthogonal frequency-division multiple access (OFDMA).

Following [HYS20], the RIS configuration can be obtained by means of 3D beam broadening and flattening, namely by partitioning the RIS into multiple sub-arrays of smaller size and optimising their phase shifts to shape one single flattened beam whose beamwidth can be properly tuned to match the size of the target subarea. The BS precoder is set to maximum ratio transmission on the equivalent channel. The RIS deployment problem is solved by block-coordinate ascent and fractional programming relaxation.

Results and outcomes

We consider a realistic indoor scenario, namely the Rennes train station in France, which is depicted in Figure , and demonstrate that our approach achieves outstanding results to improve the existing cellular infrastructure of one of the major European operators and solve the dead-zone problem, as shown in Figure . On the left-hand side we show the SNR heatmap without the RIS, whereas on the right-hand side for the case of 4 RISs, located at the square dots.

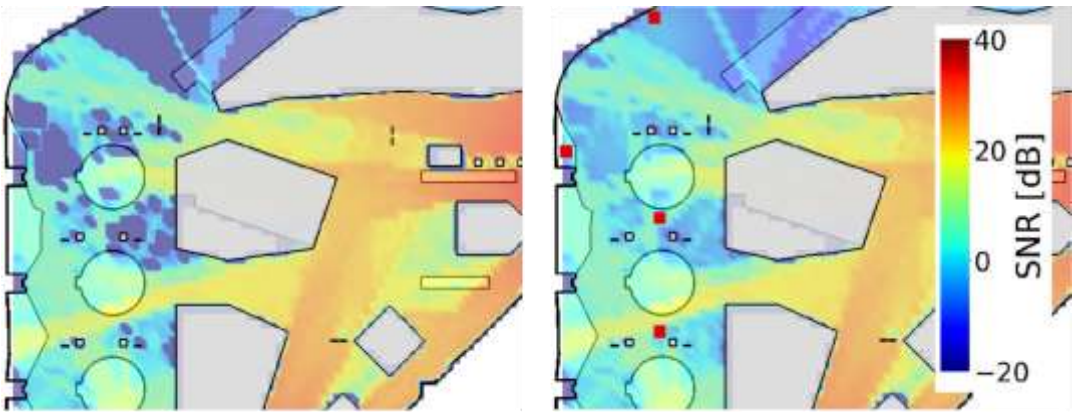

Figure 3-4: SNR heatmap without RIS (left-hand side) and with 4 RISs represented by red squares (right-hand side).

Perspective and relation to other WP4 contributions

This method provides a useful tool to optimise RIS deployment for many relevant practical scenarios. The existence of a control architecture (as developed in WP4) may be seen as an additional constraint to be included in the RIS planning algorithm.

3.3.2 Contribution #A-1: RIS-Enabled Beamforming for IoT Massive Access

Motivation and context

In [MSG21], we focus on the joint optimisation of the BS active beamforming and RIS passive beamforming by proposing an objective function, which allows to derive high-performing solutions while guaranteeing efficiency and scalability. Interestingly, the chosen metric, i.e., the SMSE, reveals a convex structure in the two optimisation variables separately, namely the precoding strategy at the transmitter and the RIS parameters. This allows to design very efficient iterative algorithms for RIS control. Specifically, we present RISMA, a RIS-empowered Multiuser Alternating optimisation algorithm that jointly optimises the beamforming strategy at the transmitter (a BS) and the RIS parameters to provide high-bandwidth low-cost connectivity in massive IoT scenarios. In marked contrast with prior work, RISMA exploits the convex nature of the problem at hand in the two optimisation variables separately to ensure scalability, efficiency, and provable convergence without the need of setting any system parameter.

We consider the scenario described in Figure , where a BS equipped with M antennas serves a set of K single-antenna UEs. The connection is established with the aid of a *nearly-passive* RIS installed on the building glasses consisting of N equivalent antenna elements. Focusing on the downlink data transmission, the BS communicates to each UE k via a direct link which comprises of a LoS path in addition to a multipath NLoS link. Additionally, the BS can exploit a combined link from the BS to the RIS which in turns reflects the incoming signal towards the UE. The latter is decomposed into the LoS BS-RIS path plus a set of scattered NLoS paths and the RIS-UE k link, which comprises of a LoS path plus a multipath NLoS link. All channels follow a quasi-static flat-fading model and thus remain constant over the transmission time of a codeword. We further assume that perfect CSI is available at the BS. The BS operates in time-division duplexing mode, such that the uplink and downlink channels are reciprocal. The downlink channel can thus be estimated through the uplink training from the UEs via a separate control channel.

Figure 3-5: Multi-UE RIS-empowered wireless network scenario.

Methodology

We formulate the problem of minimizing the SMSE of all UEs in the system by optimising both the BS and RIS active and passive beamforming configurations, respectively. For a given configuration of the

RIS, the considered system in the downlink is a broadcast channel and duality between broadcast and uplink multiple access channel holds. In the dual multiple access channel, the classical relation between MSE and maximum SINR of each UE holds for linear filters [HJU09]. Hence, this motivates us to study the SMSE to optimise the system sum rate in the downlink.

Interestingly, the problem at hand is convex in the two optimisation variables separately. Hence, by exploiting alternating optimisation we devise an optimisation algorithm dubbed as RISMA, that iterates until convergence between two closed form solutions, namely the BS active beamforming and the RIS passive beamforming. Moreover, RISMA is adapted to accommodate practical constraints when using low-resolution RISs that are comprised of antenna elements that can be activated in a binary fashion. To address this scenario, we propose Lo-RISMA, which decouples the optimisation of the binary activation coefficients and the quantized phase shifts. The former is optimised via semi-definite relaxation while the latter are projected onto the quantized space.

Results and outcomes

This framework is applied to the context of coverage enhancement by demonstrating how the use of RIS allows to increase the coverage area for a given target performance. We assume that $K = 12$ UEs are randomly distributed on a circular area of radius R_N and centered at the BS. In Figure , we assess the performance of the proposed RISMA approach in terms of sum rate versus the radius of the network R_N and for different values of transmit power P at the BS. We compare RISMA against conventional MMSE and ZF precoding (see [PHS05] and [SSH04], respectively), i.e., two state-of-the-art precoding solutions without the use of RISs, illustrating the gain obtained by the proposed method.

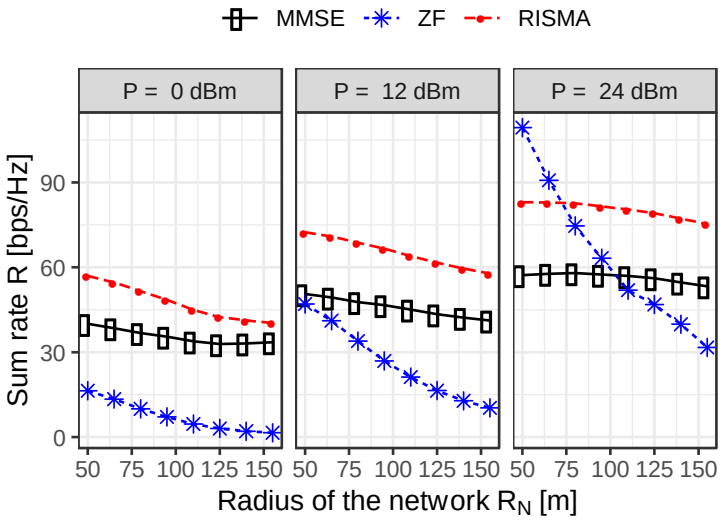

Figure 3-6: Average sum rate obtained with the proposed RISMA algorithm and with conventional MMSE and ZF precoding versus the radius of the network area and for different values of transmit power.

Moreover, we demonstrate how with even few quantization bits the achieved performance (Lo-RISMA) is nearly as good as the ideal case (RISMA) and always superior to the reference schemes.

Perspective and relation to other WP4 contributions

This contribution provides an upper bound as to what is the achievable performance of RIS-empowered networks and can thus be used as reference by other WP4 contributions.

3.3.3 Contribution #A-2: RIS-Empowered UAV Communications for Robust and Reliable Air-to-Ground Networks

Motivation and context

We consider on an air-to-ground network where UAVs are provided with passive RISs to support first responder teams in selected target areas. We propose a novel approach dubbed as *RiFe*, which considers the statistical properties of unwanted UAV oscillations due to meteorological phenomena while optimising RIS parameters such as phase shift and reflection coefficient [MDS21]. Our approach aims at tackling such undesired oscillations while steering signal reflections to build a robust and reliable air-to-ground network solution. Since UAV flight perturbations are always present and inevitable in real-life situations, RiFe aims at maximising the worst SNR averaged over the unwanted perturbations on the UAV in a target area wherein several receivers are present. RiFe is based solely on second-order statistics of said perturbations and of the position of the receivers. Thus, an advantage of such approach is the reduction in the overhead necessary to acquire instantaneous channel information. In addition to the optimisation framework, this approach is extended to account for practical considerations such as the need to update the RIS parameters due to rapidly changing channel statistics, the mobility of the UAV as well as complexity issues, and is renamed as Fair-RiFe.
As depicted in Figure , we consider a BS, or general transmitter, located at the origin of the coordinate system and equipped with multiple antennas whose signal shall cover a target area wherein first responders and/or victims are present. Moreover, we consider a *nearly passive* RIS mounted on a UAV and reflecting the signal coming from the BS towards the target area. Specifically, each receiver shall be reached by a signal experiencing a minimum SNR to successfully decode the upcoming packets. We assume that the position of the first responder team is known with some uncertainty, whereas only a probability distribution function (pdf) of the spatial position of the victims is known.

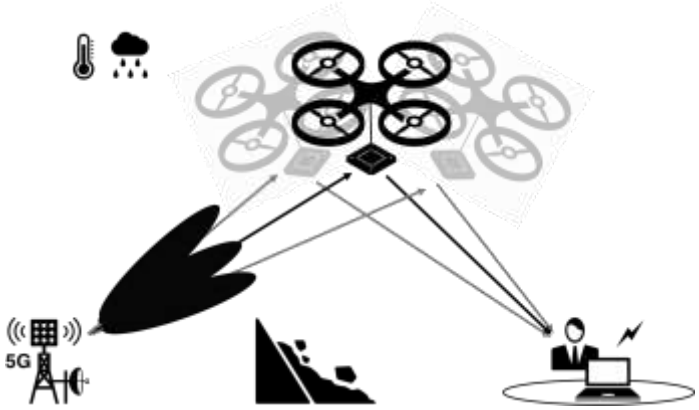

Figure 3-7: Nomadic RIS on-board UAV scenario.

Considering that the UAV is hovering, it might be subject to perturbations due to the wind or other meteorological phenomena, which result in undesired roll, yaw, and pitch of the surface of the RIS. We assume that such rotations are mutually independent and normally distributed with zero mean and given variance. We further assume that the BS has the perfect knowledge of their statistics. Given the position of the RIS with respect to the BS and the target area and the fact that we assume the drone to be maneuvered by first responder teams, the communication link between the BS and the RIS is assumed to be in line-of-sight condition with a very high probability (see, e.g., [LDY20]).

Methodology

Our objective is to guarantee coverage over a given target area, i.e., ensuring that each receiver obtains a sufficiently high SNR, by taking into account the undesired rotations of the surface of the RIS caused by perturbations on the UAV. In this regard, we consider the received SNR at a given target location and formulate an effective optimisation problem that pursues the worst SNR maximization among all possible

target locations, accounting for possible perturbations. We therefore provide a solution to such problem based on semidefinite relaxation and Monte Carlo sampling, denoted as RiFe.
We further propose a more practical solution aiming at simplifying the optimisation procedure described above. Specifically, RiFe requires to be solved every time the statistics of the perturbations are no longer valid which, given the need to use semidefinite programming, can be excessively time-consuming when the statistics change rapidly. This motivates us to propose a sub-optimal, yet simpler, closed-form solution denoted as Fair-RiFe. Given a total number of sampling points in the target area, the objective is to maximise the worst SNR at those points. Hence, we fix the RIS configuration to a weighted combination of the directions of arrival of such points. The weights need to be chosen such that more power is allocated along the propagation directions corresponding to the points exhibiting the worst SNR values.

Results and outcomes

We evaluate the minimum SNR over a given target area and average over multiple independent realizations, obtained with the proposed RiFe approach and with an agnostic solution that does not consider UAV perturbations (and thus it is not robust to them).

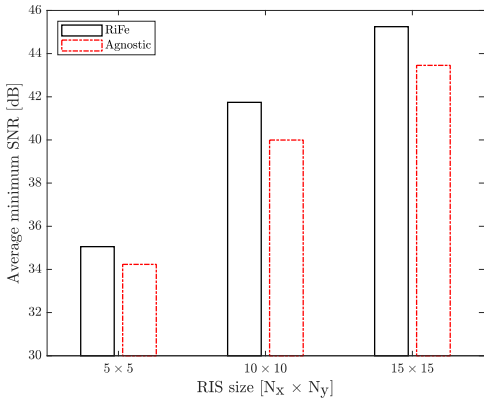

Figure 3-8: Average minimum SNR over the target area obtained with RiFe and with an agnostic solution for different number of RIS elements.

In Figure we empirically demonstrate the performance enhancement brought by the proposed RiFe approach and how much it increases with the size (in terms of number of elements) of the on-board RIS.

Perspective and relation to other WP4 contributions

This contribution is an attempt at integrating aerial platforms such as UAVs with RISs in future wireless networks. The problem of positioning such *aerial RIS* may be studied alongside conventional RIS deployment as in other WP4 contributions.

3.3.4 Contribution #A-3: A Self-Configuring RIS Solution Towards 6G

Motivation and context

Conventional RIS deployments rely on a control channel between the RIS and a centralised controller for sharing the CSI estimated at the BS and the RIS and enabling the joint optimisation of the BS precoding matrix and the phase shifts at the RIS elements. Providing a control channel, however, requires modification to the current network architecture and might limit the agility and flexibility of RIS deployment.

Therefore, in [ADS22] we develop the concept of autonomous RIS wherein reconfigurable devices can be seamlessly plugged into the existing network infrastructure without requiring sophisticated installation procedures and that can autonomously play to enhance communications KPI. We face the problem of the self-configuration of the RIS based only on local CSI obtained through a channel estimation model lato-

sensu at the RIS, i.e., without relying on an active control channel. Once the RIS is configured, it provides additional high gain multipath components between the BS and the UEs. The additional reflected paths can be detected by the standard channel sounding procedures involving BS and UEs devices, and exploited with classical methods of precoder optimisation, thus making the presence of the RIS completely transparent to the network. The main goal of this study is to analyse the feasibility of autonomous RIS deployments and compare their performance with centralised optimisation strategies.

Methodology

To acquire CSI information at the RIS, we consider a quasi-active hardware architecture comprising an array of hybrid meta-atoms, which can simultaneously reflect and absorb (i.e., sense the power of) incident signals [AAS21], [ASA21]. In the considered architecture, each RIS (metasurface) element is coupled with a sampling waveguide that propagates the absorbed (i.e., sensed) power of the incident EM waves towards some downstream RF hardware for enabling signal processing.

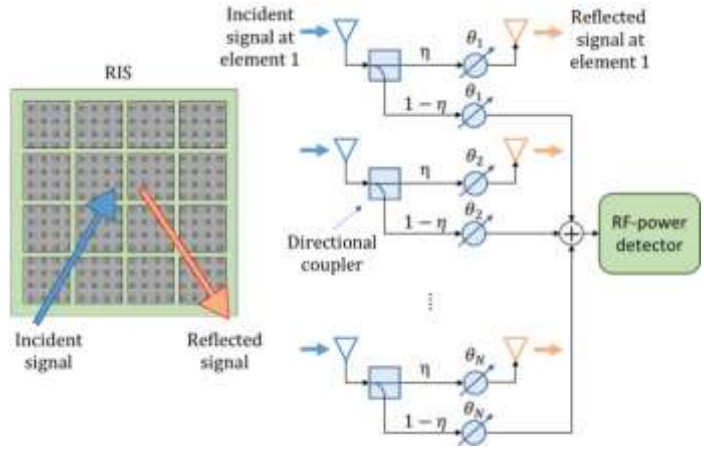

Figure 3-9: Hardware architecture inspired by [ASA21].

To reduce the complexity and cost of the required hardware, the proposed devices are not equipped with fully-fledged RF chains but only with an RF power detector, thereby eliminating the need for a receiver. The proposed hardware architecture is depicted in Figure 3-9, where the signals absorbed by each RIS element are summed together through RF combiners, which can be implemented as lumped components of the RIS RF circuit, and fed into an RF power detector that converts the RF power into a measurable DC or a low frequency signal.

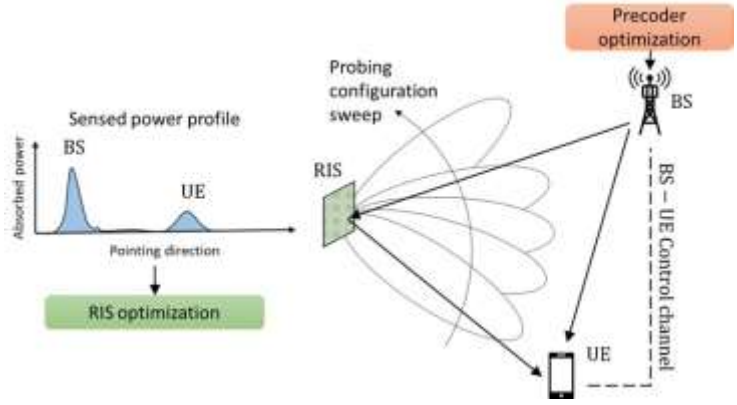

Figure 3-10: Proposed scheme for joint probing and communication

The configuration of the RIS requires the estimation of the CSI of the BS-RIS and RIS-UE channels. To this end, we devise an online optimisation approach, dubbed as MARISA, which relies upon a finite set

of RIS configurations, namely a codebook that can be iteratively tested for probing a finite set of predefined AoA, as illustrated in Figure 3-10. This operation may have a detrimental impact on the network operation, as a given RIS configuration may be in use for assisting the data transmission between the BS and some of the UEs. Therefore, changing the RIS configuration for sensing may negatively affect the communication performance. We address this issue by means of a simultaneous hybrid probing and communication scheme, as detailed in the following.
To execute the probing phase, we consider spatially directive codewords populating the codebook to maximise the absorbed power only in correspondence of a (narrow) solid angle. Accordingly, by iteratively sweeping across all the codewords, the RIS performs a scan of the 3D space, and measures the absorbed power. During this probing phase, the RIS collects a set of power measurements and obtains an angular power profile, whose peaks identify the angular directions corresponding to the position of the devices. By construction, in fact, the RIS detects a power peak only if there is at least one transmitter in the direction synthesized by the RIS beampattern. Upon completion of the probing phase, the RIS enters the communication phase, which is aimed to assist the reliable transmission of data between the BS and the active UEs, as well as to probe the 3D space to discover new UEs. Once AoAs are obtained, the local CSI at the RIS aid the BS and the active UEs with a reflected path to communicate with each other.

Results and outcomes

To assess the performance of the self-configuring RIS, and verify its feasibility, we consider a squared 50 x 50 meter service area wherein a single BS and a single RIS are located in the midpoint of adjacent edges. We consider uniform UEs distribution. We compare the performances of our self-configuration scheme against a centralised approach that jointly optimises the RIS configuration and BS precoder with perfect CSI availability.

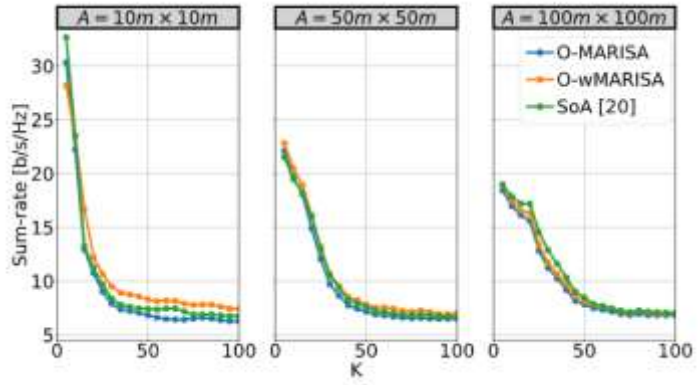

Figure 3-11: Average sum-rate in a multi-UE scenario obtained with RIS self-configuration strategy against centralised joint RIS and BS pre-coder optimisation.

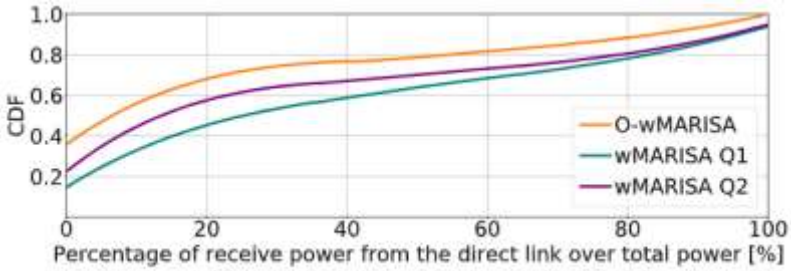

Figure 3-12: Cumulative distribution function of the fraction of the receivde power at each UE over the direct path with respect to the total received power after precoder optimisation at the BS.

Figure 3-11 provides the performance in terms of the sum rate obtained with the proposed self-configuration scheme (referred as MARISA) against the centralised approach that jointly optimises the RIS configuration and the BS precoder, while Figure 3-12 depicts the fraction of power transmitted over the additional reflected path. The results demonstrate that the proposed approach provides near-optimal sum rates when compared to fully CSI-aware benchmark schemes that rely on a dedicated control channel.

Perspective and relation to other WP4 contributions

The contribution shows the feasibility of RIS self-configuration strategies without involving a centralised controller, providing an agile deployment strategy which is in line with the work package objective.

3.3.5 Contribution #A-4: RIS-empowered Mobile Edge Computing

Motivation and context

This section considers a novel methodology for mobile edge computing empowered by multiple RISs [DMC21]. The architecture considers an access point (AP) connected to an edge server (ES) via a high-speed backhaul link, multiple UEs, and multiple nearly-passive RISs, as shown in Figure 3-13: RIS-empowered Mobile Edge Computing. The aim of this architecture is to enable edge computing services (e.g., computation offloading) to UEs, hinging on the presence of several RISs. Time is divided in slots, whose duration is designed with respect to the channel coherence time. Also, each slot is divided into two portions. The first portion of the slot is dedicated to channel estimation and control signalling, which are necessary to perform a dynamic optimisation of radio (i.e., power, transmission rates, sleep mode and duty cycle) and computation resources (e.g., CPU clock frequencies, etc.), jointly with the optimal selection of RIS's phase profiles [DMC21]. The second part of the slot is then dedicated to the actual computation offloading, which involves uplink transmission, data processing at the ES, and the downlink of results.

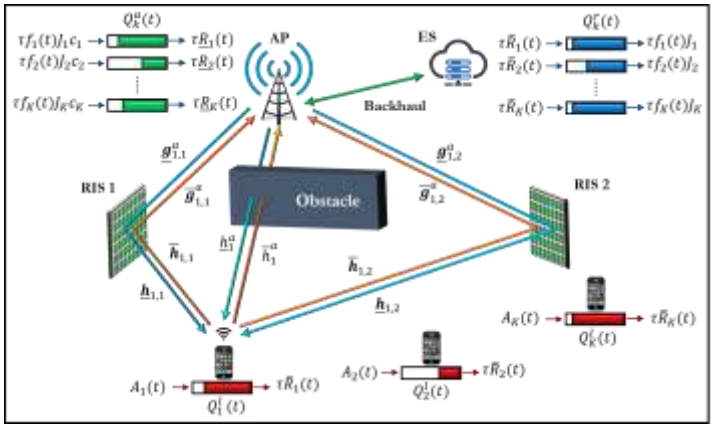

Figure 3-13: RIS-empowered Mobile Edge Computing

Methodology

RIS-empowered edge computing is performed as follows:

1. At the beginning of the slot, UEs perform a computation offloading request, which is acknowledged by the AP and the ES, if sufficient resources are available.
2. All UE-AP and UE-RIS-AP channels are estimated and transmitted to the ES.
3. The ES performs the joint optimisation of radio and computation parameters, jointly with the RISs phase shifts.

4. The ES sends the optimisation results to the AP, to the UEs (via the AP), and to RISs via a dedicated out-of-band control channel.
5. The UEs send uplink data to the AP, which is then forwarded to the edge server.
6. The edge server performs the computations required by the UEs.
7. The ES sends the computation results to the AP, which finally sends downlink data to the UEs.

The method has also been extended in [AMD22] to incorporate MIMO communications and robustness to intermittent mmWave links. In this setting, we are specifically interested to mmWave communications that imply a higher sensitivity to the presence of blockages. The main goal is to explore how effective is the use of an RIS to counteract the complexity brought when going higher in frequency and to minimize UE's transmit power, with guaranteed finite E2E delay of the offloading service. To this end, we propose an algorithm through which we investigated the dynamic joint optimisation of computing resources and RIS-empowered multiuser MIMO communication parameters, upon a blocking-aware framework. We formulate a long-term optimisation problem aiming to ensure a bounded end-to-end delay with the minimum UE's average transmit power, by jointly selecting uplink user precoding, RIS reflectivity parameters, and computation resources at the ES. Using the theory of Lyapunov stochastic optimisation, we split the long-term problem into consecutive deterministic optimisation problems, based on instantaneous observations of context parameters. Then, in each time slot t, we define a radio resource allocation sub-problem, including the optimisation of user covariance matrices and RIS parameters, and a computation resource allocation sub-problem. From a radio perspective, the problem is solved while building on an alternating optimisation strategy that couples a projected gradient step for the RIS parameters, and a water-filling solution for the users' precoding. From a computation perspective, the resource allocation sub-problem is solved with a low complex algorithm serving to optimise the ES CPU scheduling.

Results and outcomes

To evaluate the performance of the proposed architecture and optimisation strategies, we consider the following two scenarios:

- *Single-user case:* a UE performs computation offloading with the aid of one RIS. Then, in Figure 3-14: Delay-Energy trade-off in RIS-empowered MEC, we illustrate the E2E delay as a function of the user energy consumption needed to perform computation offloading, comparing a scenario without RIS with the case where one RIS is exploited, considering also imperfect channel state information (CSI) with estimation signal to noise ratio equal to η. As we can notice from Figure 3-14: Delay-Energy trade-off in RIS-empowered MEC , the proposed method exploiting RISs largely outperform the case without RIS in terms of energy-delay tradeoff.

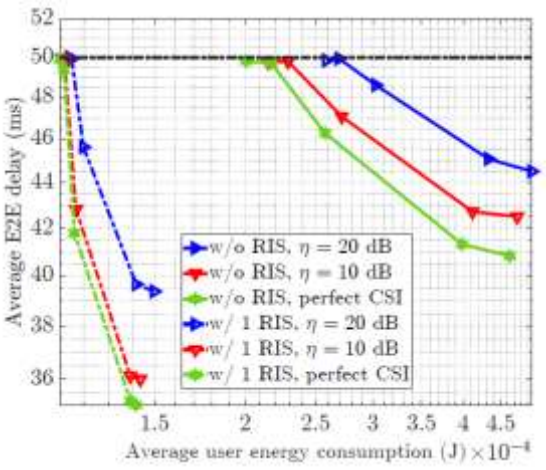

Figure 3-14: Delay-Energy trade-off in RIS-empowered MEC

- *RIS-empowered MEC over Intermittent mmWave Links:* To assess the performance of the proposed methodology in striking the best trade-off between energy consumption and delay for different blocking conditions, we compared scenarios with and without RIS. We assumed purposely, two different degrees of channel knowledge: (i) a reference strategy where instantaneous knowledge of blocking states is assumed; and (ii) a second one where only a statistical knowledge of the blockage is assumed (blocking probabilities instead of states). Furthermore, for all cases, we also consider the case in which the RIS phase shifts are randomly selected, while for radio resources allocation, we consider the case in which, the RIS phase shifts are quantized with 2 bits, which is a practical constraint of RIS implementation. The resulting delay-energy trade-off curves are shown in Figure 3-15: Delay-Energy trade-off for different offloading strategies.

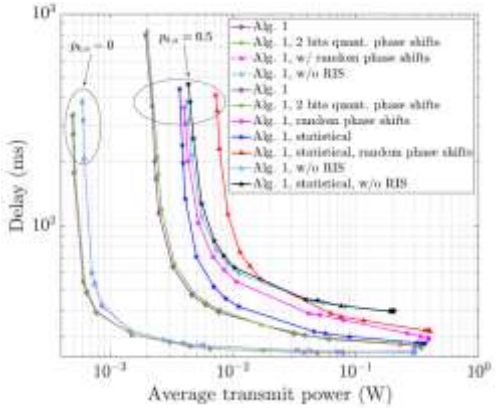

Figure 3-15: Delay-Energy trade-off for different offloading strategies

From Figure 3-15: Delay-Energy trade-off for different offloading strategies, we notice how the use of an RIS is prominent to satisfy a reliable MEC-based offloading task, while assuming different degrees of channel blocking knowledge along with different scenarios. All scenarios with optimised RIS outperform the case without RIS, although with negligible gain in the absence of blocking. This suggests that the benefits of the RIS are more significant in case of high blocking probability of the direct link. The method illustrates also very good performance if the RIS phase shifts are quantized with 2 bits, which is typical of practical scenarios.

Perspective and relation to other WP4 contributions

The method allows for several generalisations, spanning from the incorporation of sophisticated RIS channel models to the definition of the specific applications running at the edge server. The method hinges on the RIS channel estimation methods developed in WP4.

4 RIS control methods

The communication in a generic wireless system depends on various operations required before the actual transmission of the data can take place. In a generic network, the activities to be performed include channel estimation, allocation of transmission resources, and adaptation of the transmission parameters. In addition to this, RIS-empowered systems need to consider the procedures for configuring the RIS elements, in connection with the aforementioned tasks. We organise the possible task performed by the network in Table 5, where we group various operations in five phases: initialisation; sensing and channel estimation; resource and RIS configuration optimisation; metric measurement; data transmission. Note that the order of these phases may vary depending on the communication aim.

The actual performance of a RIS-empowered communication system is strictly related to the design of control methods, which defines the exchange of information between the various operations required for the communication. We remark that all phases are influenced by the kind of RIS hardware, control channel and ownership, as defined in Section 1.3. An overview is given in the following.

- **Hardware.** Nearly-passive, quasi-active and active RISs have different sensing capabilities, and thus their influences on the CE phase; also, active RISs can use their transmission capabilities for metric measurements in the MM phase.
- **Control channel.** Between the explicit control channels, in-band and out-of-band CCs play an important role when considering the ALG phase; in particular, in-band control channels require a reliable communication between RIS controller and RIS hardware, impacting on the choice of resource allocation and RIS configuration. This constraint is relaxed for the out-of-band channel, leading to a simpler control design. On the other hand, the possibility of optimising both control and communication parameters may lead to higher performance[2].
- **Autonomous or controlled RIS.** Autonomous RISs require low to zero explicit control. When needed, the control information regards mostly synchronization signaling, while the main operations are taken at the RIS itself. On the other hand, controlled RISs require detailed control information to work as intended.
- **Ownership.** Depending on the kind of ownership, the methods designed to take control and use of the RIS change. In general, coordination between controlling entities is needed to avoid unwanted interference to end-users served.

In the following, we consider the above aspects to discuss the requirements for control and signaling.

Table 5: Definition of the general phases needed for RIS-aided communication networks

Phase	Label	Example of tasks involved	Considerations
Initialisation	INIT	Device connection; UE identification; Specification requirements (KPIs, communication type, etc.).	Access procedures can influence or can be influenced by localisation algorithms.
Sensing and channel estimation	CE	Exchanging of pilots; collection of sensing measurements (channel coefficients, RSSI, etc.); performing estimation of parameters.	RIS hardware deeply influences sensing capabilities, impacting on the CE protocol design.
Resource and RIS configuration optimisation	ALG	Performing power, resource and beamforming allocation at BS/UE; RIS configuration optimisation/selection according to an objective/algorithm	Protocol design is influenced by the point in the transmission chain where processing is performed (MEC, BS, controller, etc.)
Metric measurement	MM	The UE (DL)/BS (UL) measures the relevant KPIs; feedback is provided to the RIS controller.	Possible feedback can be: KPI value; ACK/NACK, depending on satisfaction threshold; ACK if threshold is satisfied, no transmission otherwise. Type of CC influences the choice of metric measurement.
Data Transmission	DT	UL/DL transmissions take place with the selected RIS configuration.	

4.1 Algorithmic requirement for RIS operation

The algorithmic requirements for RIS operation are generally related to channel estimation, scheduling, and configuration. However, the specifics and who bears the responsibility depends on whether the RIS operates autonomously or is being explicitly controlled (with the latter scenario typically offering more capabilities and flexibility at the cost of higher control overhead):

- *Controlled RIS* – in non-autonomous RIS (managed by BS-side controller or RISO), the algorithmic requirements are primarily placed on the respective BS or RISO. One such requirement

[2] Implicit control channel is not addressed here, being not relevant for this section.

calls for novel channel estimation procedures that consider the specifics of composite channels (explained in more detail below). Other algorithmic aspects are related to resource allocation and scheduling techniques that are RIS-aware. Whenever feasible, the objective should be to jointly optimise RIS configuration and the transmission parameters of BS/multiple UEs. Further algorithmic nuances appear when RIS needs to be shared by multiple operators/stake holders. In that case, additional constraints on the scheduling as well as cross-interference (related to the bandwidth-of-influence) need to be taken into account.

- *Autonomous RIS* – when RIS operates autonomously (either natively or as one of its modes, i.e. upon being instructed by the external controller to act autonomously until further notice), the algorithmic requirements include: capability to obtain and process channel measurements locally; ability to determine appropriate configuration based on locally implemented algorithm (through e.g. machine learning or other optimisation techniques); being able (to some extent) to infer the communication objective and self-adjust, e.g., by detecting pilots specific to localisation and/or sensing, it might use different set of configurations to facilitate those procedures.

4.1.1 Channel estimation procedures

A big portion of the algorithms designed for RIS control and orchestration are designed to utilise Channel State Information (CSI) to achieve their intended objectives. In fact, the problem of reliably estimating information about channels when RISs are introduced is more challenging [WHG22], [JAS22], [JAB22]. Firstly, it involves the estimation of multiple channels simultaneously (the direct channel between the BS and each UE, the channel between the RIS and BS, and the channel between the RIS and each UE). Moreover, the dimension of the channel matrices for estimation increases with the number of RIS elements. In addition, the standard end-to-end pilot-exchange method results to measurements of the cascaded channel instead of the aforementioned links. Lastly, the near-field channel estimation problem needs to be taken into consideration which is a fundamentally different process. This task becomes more complex when the deployed RISs are equipped with massive elements with non-linear hardware impairments [HHA20], [SDE19]. The unavoidable hardware error decreases the accuracy of channel estimation (CE), and the beam squint phenomenon occurs in wideband channels. To that end, the deployment strategies and control protocols of RIS based environments must take the CE step into consideration.

In general, the CE process involves the transmission of (predominantly known) pilot symbols or information from the sending node to the receiver, at which end, an estimation process is performed. When RISs are involved, multiple pilots are sent, while the RIS changes its configuration to collect descriptive data about the channel. Such a protocol is described as a separate contribution in Section 4.4.2. From a CC perspective, the RIS may either change its configuration autonomously, provided sufficient synchronisation (Implicit CC), or may be controlled to desirable configurations during the estimation process (Explicit CC – either in-band or out-of-band). It is important to mention that the above framework is only able to measure the cascaded channel instead of the individual links, due to the reflective-only capabilities of the standard RISs. However, many RIS control algorithms rely heavily on the knowledge of the separate component channels. To that end, a separate contribution is described in Section 4.4.3 that utilises the sensing capabilities of a quasi-active RIS to estimate the individual BS-UE and UE-RIS links.

Finally, let it be noted that a parametric CE procedure is an alternative to the direct measurement estimation using pilot exchanges. In this context, the CE task of the RIS communication protocol involves measuring certain components of the network (e.g., angles of departure from the sender to the receiver), which can be exploited under sensing frameworks. As such, those methods will be predominantly studied in Work Package 5 of this project.

4.1.2 Computational resources

The algorithmic control of the RISs necessitates several additional requirements. At first, the network needs to be empowered with computational capabilities. The specific requirements of the computational infrastructure depend on the exact application scenario, although in principle, the computation may happen at either communication end, the BS, or at the RIS controller, perhaps aided by a MEC server. An-

other consideration of multi-user systems is whether the employed algorithms are designed in a distributed or in a centralised manner. The latter case has the potential for higher performance, but it requires additive information exchange operations between the involved nodes.

4.1.3 KPI measurement

An important consideration of RISE environments is the ability to compute the metric of interest at certain instances. The reason behind this is twofold. On one hand, the resulted KPIs can be used to evaluate the performance of different proposed algorithms and strategies. More importantly, autonomous deployment strategies (such as the contribution of Section 4.4.5) mostly rely on continuous observations of the current KPI value, as a feedback signal. This entails both a measuring and a signaling overhead.

For the metrics considered here, the receiving end node is capable of individually performing the computation of the current metric value without the need for explicit communication with the sender (or with only minimal communication that can be carried out during the access phase). Moreover, the metric values can also be computed without complex infrastructure requirements (e.g., channel measuring or sensing). On the other hand, the KPI measurement may introduce a signaling overhead since the measured values need to be transmitted to the computation-capable part of the network.

4.2 Access procedures for RIS-empowered systems

The presence of a RIS in a network influences the access procedures considered. These procedures should take into account the initial access of UEs, and the access to the RIS controller, if present, to control the operation of the RIS.

4.2.1 **UE initial access**

For the UEs initial access in absence of any information, the procedure may be done sweeping through a set of possible configurations of the RIS [CSL22]. Using a training (DL) phase we let the UEs learn which configuration provides a sustainable SNR. Using this information, each UEs can send pilot signals during the access (UL) phase in the attempt to access the network. An example of data exchanged for performing the access is given in Section 5.1.

The correct implementation of the access protocol requires a careful design of the pool of configuration used. These must be planned considering both the coverage of the area of interest and the time needed for training and access phases. A high number of configurations translate into a larger covered area, but also into a higher time needed for sweeping through them, possibly reducing the overall throughput. A trade-off must be found depending on the scenario at hand. We remark that the use of configuration having large beamwidth (e.g., as [JNS21]) might be beneficial for this task, especially when expecting a low number of UEs accessing at once. A more selective beamformer gives advantage for crowded scenarios, being able to separate them in space, thus reducing the collision probability.

4.2.2 **Accessing RIS controller**

To control the operations of the controlled RIS, specific procedures and data frames must be designed. In general, an entity of the network (usually the BS) connects to the RIS controller in order to instruct a configuration change, carefully evaluated using optimisation and/or machine learning methods.
A possible control frame for this task should have at least the following fields:

- *element ID:* the information on the group of RIS elements that needs to change their phase shift profile. This can be avoided if the RIS always reconfigure all its elements.
- *configuration profile:* either phase or amplitude parameter (or both) of the elements involved in the configuration change. The resolution of the RIS, i.e., the number of levels that each RIS element can take, directly affects the length of this field. It should be noted that in the system there might be multiple RISs with different resolutions, which will entail configuration packets of variable lengths.

Moreover, we can always assume that the RIS control has memory capabilities, and it can store some configurations in a look-up table. In that case, additional fields can be considered into the control frame:

- *Overwrite:* flag denoting whether the provided configuration should be saved locally in the look-up table at the RIS controller.
- *Configuration no.:* if *Overwrite = "true"*, it denotes the index in the look-up table under which the configuration is stored; since the number of possible configurations is potentially huge, only a limited subset might be preserved.

If a configuration profile is stored into the look-up table, it may be convenient to inform the controller to load it, transmitting only the Configuration no., thus reducing the control information required. Hence, the control packet can be either in the "long" or in the "short" format. To enable this possibility, a flag informing the Type of control packet should be inserted in the header of the frame. Figure and Figure show a representation of both short and long control frames.
We remark that in case of a wireless control channel, particularly in-band, the use of short packets is the preferred choice to increase the reliability of the control transmission.

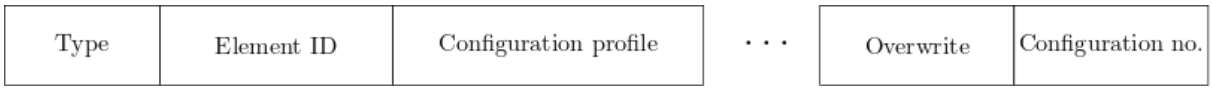

Figure 4-1: Long control packet for configuration profile

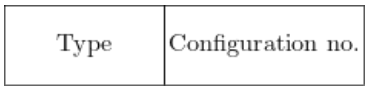

Figure 4-2: Short control packet for configuration profile

Finally, other kinds of control information is required if the controller can locally run an optimisation procedure. In this case, the information required depends on the specifications of the optimisation algorithm. In general, we can divide the requirements in two:

- channel and environment information, if the algorithm is based on CSI for optimising the channel reflection coefficient.
- measurement of KPIs (i.e., SINR at the receivers), if the algorithm modifies the policy after checking the results in the environment; this is particularly suitable for machine learning approaches involving feedback, such as reinforcement learning techniques.

For this information type, the control channel can be designed according to the transmission of CSI and KPI data, as a conventional control channel used in the 5G NR standard. Here, particular attention to the reliability must be taken into consideration for in-band control channels.

4.3 RAN protocol structure with in-band and out-of-band signaling

As already mentioned, the type of control channel affects the protocol structure. When the explicit out-of-band control channel is present, the protocol structure must take into account only the exchange of information needed to perform the communication task. Indeed, the control information for the RIS is not influenced by the communication data.

In presence of the in-band control channel, the entity acting as controller needs to keep a communication channel open towards the RIS every time a control packet must be sent. From another point of view, spectral and temporal resources must be allocated (and communicated to the RIS) to provide a reliable communication between controller and RIS. Moreover, the RIS must have locally the optimal configuration profile to be used when receiving control packets. Otherwise, the control packet may be lost due to beamforming mismatch. Accordingly, the deployment of the RIS with in-band channel is subject to a special configuration phase where the CSI of the controller-RIS is estimated and used to perform the control plane optimisation. This configuration phase should be repeated according to the time coherence

of the channel. We remark that control CSI estimation may be performed simultaneously to the CSI estimation of users during the CE phase. By means of joint optimisation, both communication and control phases can be then optimised. It is worth noting that quasi-active and active RISs can be exploited for control plane optimisation, being able to receive (send) pilot from (to) the controller directly. Also, processing capabilities at the RIS permit to distribute the computational load for the optimisation,

4.4 Contributions

An overview of the contributions on RIS control methods from RISE-6G is provided in Table 6.

Table 6: Summary of contributions on RIS control methods from RISE-6G and the related system

Architecture	# BS	# RIS	# UEs	UE mobility	RIS mobility	LoS/NLoS	KPI	CC type
B-0: Random Access protocol based on "sweeping" through RIS configurations	1	1	multiple	static	static	NLoS between UE and BS, LoS between UE and RIS	Throughput	Explicit out-of-band
B-1: Channel estimation using parallel factor decomposition	1	1	multiple	mobile	static	NLoS (Rayleigh Fading)	NMSE	Either explicit or implicit CC
B-2: Channel estimation with simultaneous reflecting and sensing RIS	1	1	multiple	static (extensible to mobile)	static	NLoS (Rayleigh Fading)	NMSE	Explicit-out-of-band
B-3: RIS tuning in rich-scattering environments through learning the channel model with deep learning	1	1	1	static	static	NLoS with Rich Scattering	SE	Either type during data collection / No control needed during operation
B-4: Online control of RIS configurations using deep reinforcement learning	1	multiple	multiple	mobile	static	Both (Ricean Fading)	SE	Implicit out-of-band
B-5: A receive quadrature reflective modulation scheme	1	1	1	Static (extensible to mobile)	static	Both (Ricean Fading)	BER	Implicit CC
B-6: Non-coherent MIMO-OFDM utilising spatial diversity	1	1	1	mobile	static	NLoS (Rayleigh Fading)	SE, BER	Implicit CC

4.4.1 Contribution #B-0: Random Access protocol based on "sweeping" through RIS configurations

Motivation and context

Consider a scenario where users equipments (UEs) cannot be served by a base station (BS) due to blockages. To overcome this problem, a network operator can deploy a RIS to extend the coverage area of the BS and offer network access to the UEs affected by the blockages. In this setting, an important open question is how to design an access protocol for multiple uncoordinated UEs, while taking advantage of the possibility to configure the RIS. The aim of this section is to illustrate a random-access protocol based on the spatial dimension given by the RIS. The scenario of interest is given in Figure 4-3.

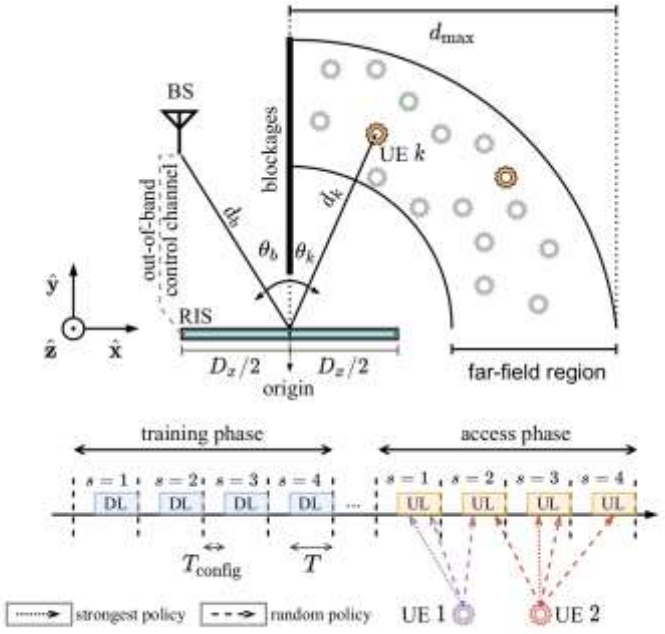

Figure 4-3: RIS-empowered downlink joint localisation and synchronization of a single-antenna UE

Methodology

The proposed protocol is divided into a DL training phase and an UL access phase, as illustrated in Figure 4-3. In the training phase, the BS controls the RIS to sweep over a finite number of configurations, one for each slot, while the UEs can estimate the importance, or "strength," of each configuration in relation to their positions by relying on training signals sent by the BS. The DL training phase is then followed by an UL access phase, where the sweeping is performed again. Active UEs now try to access the network according to access policies that exploit the side-information obtained in the training phase. Thus, the RIS helps to spatially coordinate the access requests from the UEs.
The UEs can select two different access policies:

1. *Strongest-configuration policy (SCP):* each UE chooses the access slot associated to the RIS configuration leading to the best channel quality. Consequently, each UE sends a single packet.
2. *Configuration-aware random policy (CARP):* each UE compute a probability mass function for slot selection with probabilities proportional to the strength of the receiving signal of each configuration. Then, each UE decides the access slots by tossing a biased coin with probability previously computed. Hence, each UE can send multiple replicas of its packet. The collision resolution is performed searching for singletons and performing SIC, as the classical slotted ALOHA paradigm.

Results and outcomes

As a benchmark, we use the so-called unaware random policy (URP) which does not rely on the training phase; thus, the choice of the access slot is made randomly. The results reveal a very important trade-off, shown in Figure 4-4. On one hand, the use of the RIS to coordinate the access requests from the UEs better resolves collisions, increasing the average number of successful access attempts. On the other hand, the price to pay for RIS help is increased access delay since it depends on a training phase. Remarkably, RIS-empowered policies outperform random policies when the system gets crowded.

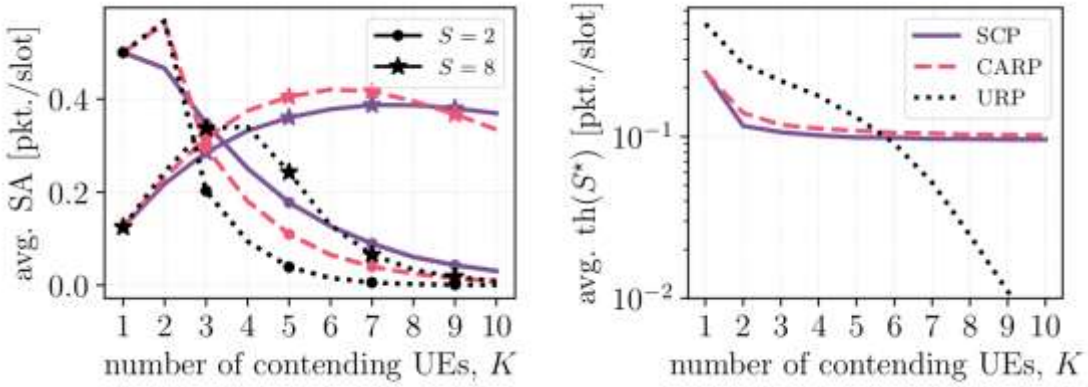

Figure 4-4: Performance of the proposed random-access protocol. Here, *S* denotes the number of configurations used. The plots show the average number of successful access attempts (left), and the optimal average throughput with respect to *S*. [CSL22]

Perspective and relation to other WP4 contributions

The proposed random-access procedure can retrieve information on the CSI of the user for every configuration of the RIS involved in the access phase. At the end of the procedure, the BS is informed on which configuration each user prefers for transmission. This information can be broadcasted to RIS profile optimisation algorithms providing a feasible initialisation.

4.4.2 Contribution #B-1: Channel estimation using parallel factor decomposition

Motivation and context

The problem of channel estimation (CE) in MIMO systems has been efficiently tackled using the PARAllel FACtor (PARAFAC) decomposition scheme [WHA21]. The scenario is depicted in Figure 4-5: The considered multi-user downlink system for channel estimation using PARAFAC.Figure 4-5: The considered multi-user downlink system for channel estimation using PARAFAC. . Since CE in RIS communications involves estimating large scale channel matrices, low complexity solutions can be devised through the application of the PARAFAC decomposition technique in this context.

Methodology

- A CE framework is introduced for multi-user MIMO systems that decomposes the high dimensional channel matrices involved into a linear combination of rank-one tensors.
- Two iterative estimating procedures are then proposed to recover the pilot signals from the noisy observations, namely:
    - Alternating least squares,
    - Vector approximate message passing.

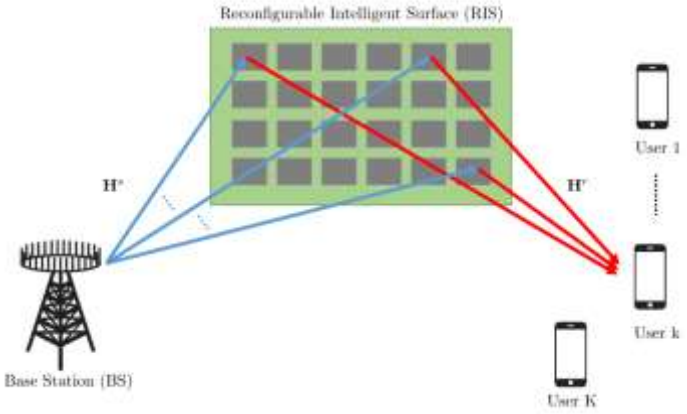

Figure 4-5: The considered multi-user downlink system for channel estimation using PARAFAC.

Results and outcomes

The proposed methodology has been validated in a downlink RIS-empowered MIMO system under different BS precoding schemes. Feasibility conditions and bounds on the performance estimation has been derived. Numerical results demonstrate that the proposed schemes outperform benchmark and state-of-the-art algorithms for CE, while exhibiting performance close to the theoretical upper bounds.

The limitations of this contribution are the following:

- Both the number of BS antennas and the number of users must be larger than the RIS elements.
- To reduce estimation ambiguity, the performance of the technique also needs to be constrained.

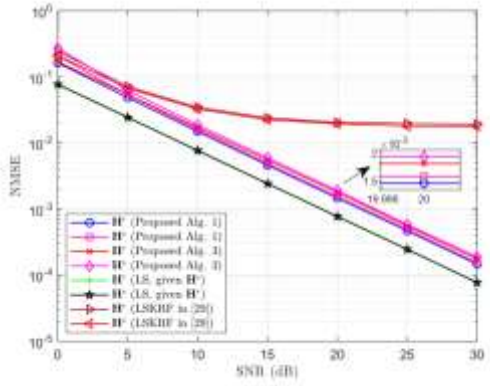

Figure 4-6: NMSE performance between the proposed PARAFRAC-based algorithms, genie-aided Least Squares (LS) estimation and the approach from [AA20].

Perspective and relation to other WP4 contributions

This technique for channel estimation reduces the computational requirements of the involved iterative estimation schemes. At the same time, it does not pose any special requirements on the RIS architecture deployed in the system. Nevertheless, more elaborate CE schemes can be involved when hybrid RIS architectures are available.

4.4.3 Contribution #B-2: Channel estimation with simultaneous reflecting and sensing RIS

Motivation and context

Since large numbers of reflecting elements are involved during the transmission process of RISE networks, the problem of CE is getting increasingly difficult and requires a considerable overhead in terms

of pilot signals and involved computations. Even more so, common reflective RISs allow only for the end-to-end channel to be estimated. This poses fundamental limitations to the application of many algorithmic frameworks that usually make assumptions about the availability of CSI on individual communication links. Those limitations, however, can be overcome by the deployment of a RIS empowered with both reflecting and receiving functionality. Those quasi-active RISs not only control the impinging waveform but are also capable of sensing and processing signals using some active elements (i.e., elements with enabled RF-chains.

Methodology

This contribution concerns the process of channel estimation in a quasi-active-RIS-empowered system. An indicative application considering an uplink multi-user scenario was studied. In that, a (controllable) portion of the impinging RF signal is absorbed by the active RF-chains to perform the local analog combining and digital processing, before being forwarded (out-of-bound) to the RIS controller. An illustration of the proposed methodology is given in Figure 4-7: Illustration of the proposed quasi-active RIS metamaterials.Figure 4-7: Illustration of the proposed quasi-active RIS metamaterials..

A lower bound of the number of power signals needed for ideal channels has been derived, and the estimation-MSE of the individual links has been expressed as functions of the quasi-active RIS parameters, given the received pilots. Therefore, the estimation procedure is facilitated using standard numerical optimisation algorithms.

Results and outcomes

In the high SNR regime, and considering the ideal case of negligible noise presence, the lower number of pilots needed for accurate recovery of the individual channel links is proved to be inversely proportional to the ratio of the total number of RIS elements versus the number of RF-enabled elements, resulting in an intuitive benefit in terms of pilot overhead when quasi-active RISs with a reasonable number of active elements are deployed. A practical consideration of the methodology is to determine the power splitting parameter of the surface. It has been observed that a trade-off in the accuracy of the BS-RIS versus UE-RIS links exists when the ratio of the reflected signal is lower than 50%, while no substantial improvements are observed after that value. As we can notice from Figure 4-8: Channel estimation performance of the proposed methodology utilising a quasi-active RIS. (left) Trade-off of estimation errors between the BS-RIS and the BS-UE links across different configurations. (right) Estimation of the cascaded channel over increasing SNR values. In the figures, the quasi-active RIS is denoted by HRIS.Figure 4-8: Channel estimation performance of the proposed methodology utilising a quasi-active RIS. (left) Trade-off of estimation errors between the BS-RIS and the BS-UE links across different configurations. (right) Estimation of the cascaded channel over

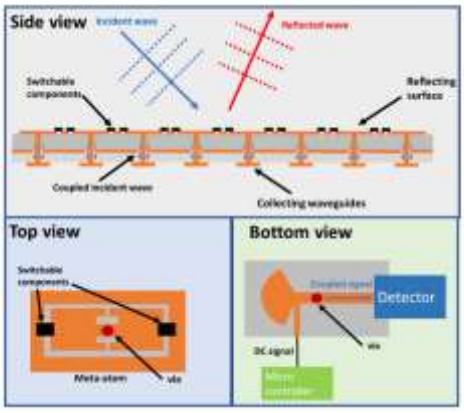

Figure 4-7: Illustration of the proposed quasi-active RIS metamaterials.

increasing SNR values. In the figures, the quasi-active RIS is denoted by HRIS., when comparing estimation results of the quasi-active RIS methodology over a benchmark approach utilizing a reflective RIS and setting the number of pilots to equal lengths for both cases, the quasi-active approach results in multiple orders of magnitude lower error in the estimation of the cascaded channel in the high-SNR regimes.

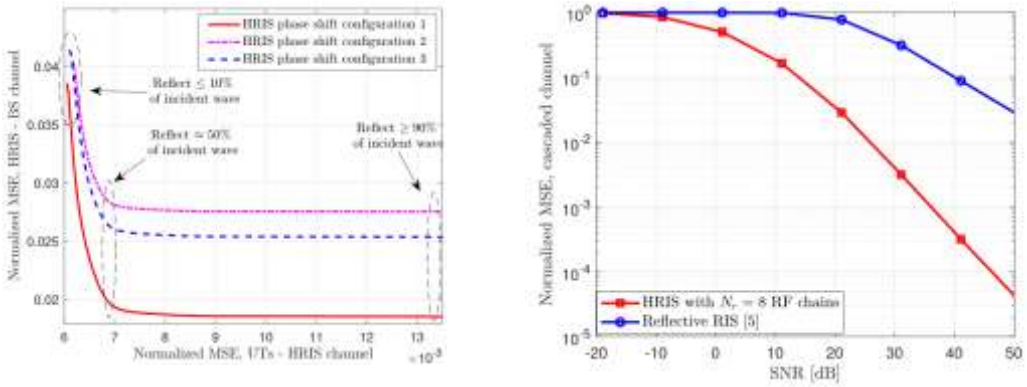

Figure 4-8: Channel estimation performance of the proposed methodology utilising a quasi-active RIS. (left) Trade-off of estimation errors between the BS-RIS and the BS-UE links across different configurations. (right) Estimation of the cascaded channel over increasing SNR values. In the figures, the quasi-active RIS is denoted by HRIS.

Perspective and relation to other WP4 contributions

The benefits of this approach are illustrated by the fact that the number of pilots needed for effective CE can be hugely decreased when quasi-active RISs with only a small number of RF-enabled elements are considered. As a sidenote, quasi-active RISs can also be configured to act in reflect-only or receive-only mode, if desired, and as a result they can be deployed with negligible control and energy overheads when their sensing functionality is not needed.

4.4.4 Contribution #B-3: RIS tuning in rich-scattering environments through learning the channel model with deep learning

Motivation and context

Rich scattering occurs in wireless environments in which many scattering objects appear. When those scatterers move through time the state of the channel changes dynamically in unpredictable patterns. As a result, it is infeasible to optimise the network's component at every time step. Nevertheless, it is conceivable that the average dynamics of the environment can be captured.

Methodology

The proposed methodology is a three-stage approach for finding the optimal RIS configuration that results in the optimal long-term (average) performance [SSH22]:

1. At the first stage, the RIS is set to random configurations and multiple-channel responses are measured and collected.
2. An artificial neural network is trained to observe a RIS configuration and predict the expected channel response. Utilising the frequency response, the achievable rate can be computed.
3. An iterative maximisation procedure is applied to find the optimal RIS profile. At every iteration, the achievable rate is computed using the trained network's predictions. A genetic algorithm was selected as the maximisation procedure to deal with the discrete nature of the RIS configurations.

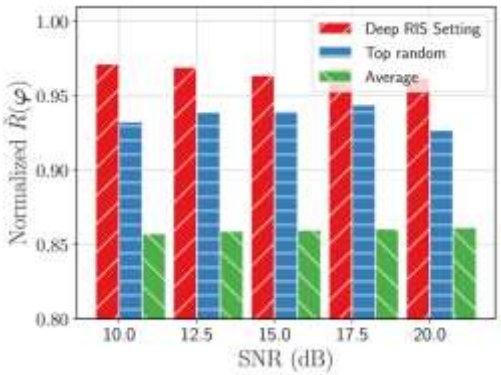

Figure 4-9: Normalised ergodic rate of the proposed "Deep RIS Setting" method as a fraction of the optimal achievable rates of exhaustive search.

Results and outcomes

A numerical evaluation process was carried out with the use of a physics-faithful simulator that constitutes a separate contribution to WP3. The deployed neural network was shown to be capable of learning the expected frequency responses of the cascaded channel. The genetic algorithm exhibits near optimal rate performance and outperforms the strategy of searching randomly through RIS profiles. An example of performance improvement is provided in Figure 4-9: Normalised ergodic rate of the proposed "Deep RIS Setting" method as a fraction of the optimal achievable rates of exhaustive search..

Perspective and relation to other WP4 contributions

This is an offline tuning method, i.e., it can be deployed prior to the final deployment of the RIS solution with no measurement, control, or computations cost during operation. A limitation of the methodology arises from the fact that in rich scattering environments the random RIS tuning achieves comparable performance to the optimised configuration.

4.4.5 Contribution #B-4: Online RIS control using deep reinforcement learning

Motivation and context

In practical applications, the wireless environment is characterized by changes and the channel states evolve over time. This dynamic nature of the environment may be the effect of users' movement, temporary blockages, out-of-network interferences, etc. In such cases, the problem of RIS tuning becomes challenging since traditional methods require solving an iterative optimisation problem at every new channel state to determine the (near) optimal RIS configuration. Evidently, such methodologies suffer from sever computational overheads. Making the RISs truly intelligent necessitates some form of learning from past experiences. For this reason, RIS control can be effectively treated through Deep Reinforcement Learning (DRL), since such algorithms can be trained on observed data, leveraging fast inference times, while also being able to adapt to temporal changes within the environment.

Methodology

We propose the use of DRL-based RIS orchestrators for real-time RIS tuning [SAH22, ASH22]. To that end, we have established a general framework that formulates the RIS control problem as a reinforcement learning problem. DRL algorithms are agnostic of the system modelling they are applied on, and they instead aim to derive optimal decision-making strategies based on available observations and feedback. In the general case, the agent (orchestrator) observes the current CSI, which prompts it to select the RIS profile (along with other parameters of the system, such as the precoding matrix in MISO systems). In downlink communications, the appropriate KPI (e.g., SINR for the multi-user case) is measured at the

UEs and is sent back to the orchestrator as a feedback signal, allowing for a training procedure to take place. The benefit of this procedure is that each decision on the RIS profile happens in real time.

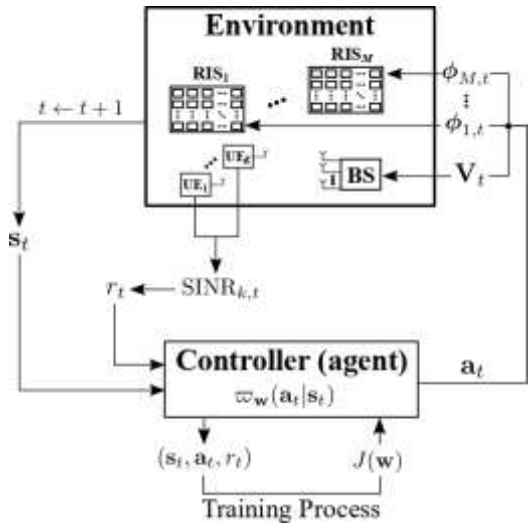

Figure 4-10: General reinforcement learning framework for RIS configuration tuning and precoder selection toward maximising the sum-SINR-rate in multi-user MISO systems.

Results and outcomes

Utilizing this formulation, we illustrate the following results. We have proposed a deep-learning-based contextual bandit algorithm for the sum-rate maximization objective in multi-user systems. This algorithm requires lower computational costs and is better-behaved with respect to state-of-the-art DRL algorithms. Despite that, numerical evaluations show that its performance is on par with the benchmarks used in the comparison. The formulation also allows for a simplified multi-armed bandit algorithm that does

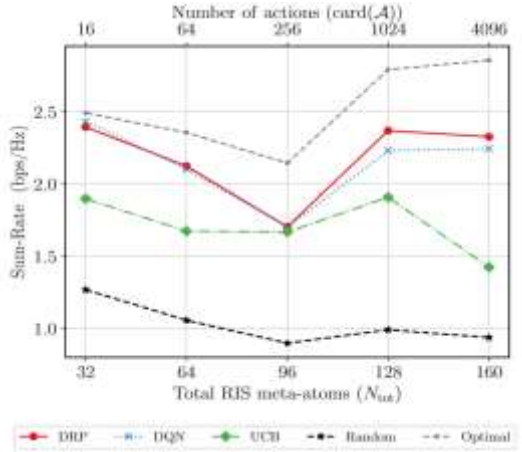

Figure 4-11: Evaluation of the proposed "DRP" algorithm in increasing RIS sizes. Its performance is on par with the more computationally expensive Deep Q Networks (DQN) benchmark. It is shown to outperform the Upper Confidence Bound (UCB) and random-configuration-selection benchmarks.

not depend on any observation, but it can rather learn to select favorable RIS configurations based only on the feedback signals, albeit with a limited efficiency as the number of configurations increases.

Perspective and relation to other WP4 contributions

Deploying DRL-based RIS orchestrators has the advantage of online adaptability to environment changes. Leveraging fast and accurate CE methods is important to the effectiveness of such methods. An

added requirement of DRL is that the communication rates need to be computed and sent to the orchestrator during the training period.

4.4.6 Contribution #B-5*:* A receive quadrature reflective modulation scheme

Motivation and context

The reflection coefficients of the RIS can also be controlled according to the information to be transmitted. Under this prism, the concept of RIS-based modulation can be introduced, in which, the configuration of the RIS is utilised to form an end-to-end spatial modulation scheme.

Methodology

A spatial modulation scheme is designed for RIS-enabled communications [YWL21]. For this operation, the reflecting elements of the RIS are (randomly) split into two halves (each comprised of $n + 1$ elements) to create the in-phase and quadrature components of the reflected signal. Each component carries a different data stream, which is then steered to a different received antenna. For each component, the first n elements of the configuration encode the number of the receive antenna this component targets while the last bit determines the positive/negative polarity of the component beam. The combined phase-shifting configuration results to a unique reflection pattern for each channel according to the information bits. Each component is steered to a different antenna, in which the intended sub-channels with the same phase result to a received signal with larger power than any other of the receive antennas. When the appropriate antenna is determined, the information bit can be decoded based on the polarity, resulting to a detector of low complexity which also dispenses with the CSI at the receiver.

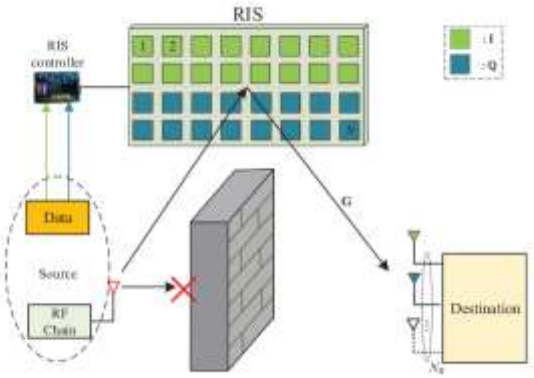

Figure 4-13: System overview of the receive quadrature reflective modulation scheme.

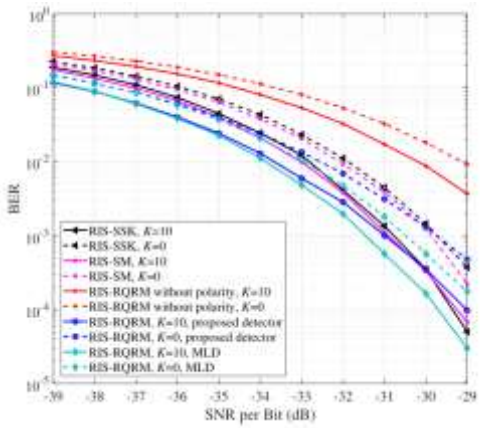

Figure 4-12: Performance comparison among the proposed methodology (termed "RIS-RQRM") and benchmarks termed "RIS-SSK" and "RIS-SM".

Results and outcomes

Approximate mathematical expressions for the average BER of the presented modulation scheme over Rician fading channels have been derived. The BER performance of this method was evaluated numerically to show that it outperforms existing RIS-centered modulation schemes in the low SNR regime.

Perspective and relation to other WP4 contributions

This specific contribution proposes a RIS-enabled system, in which the RIS is used for modulation of the transmitted data. This differs from the optimisation-nature of most of the contributions of this document.

4.4.7 Contribution #B-6*:* Non-coherent MIMO-OFDM utilising spatial diversity

Motivation and context

In typical operations, RIS-empowered systems rely on traditional coherent demodulation schemes. Those have the disadvantage of requiring CSI estimations, which is a challenging task to achieve in RIS systems.

Methodology

In this contribution a RIS-empowered OFDM system is proposed [CAG22] and studied, based on non-coherent modulation, namely the differential phase shift keying. The system under investigation is especially suited for high noise and/or mobility scenarios, in which, CE is inherently challenging.

The example system considers the uplink between a single-antenna user and a multi-antenna BS. In the proposed non-coherent demodulation scheme, the data symbols are differentially encoded in the time domain at the UE. Under this framework, only a single reference symbol at the beginning of the burst is required. The symbol detection operation is performed without the knowledge of the CSI. Let it be noted that another advantage of this system is that it does not require any configuration of the RIS.

Results and outcomes

The extensive numerical evaluation conducted verified the accuracy of the proposed methodology and demonstrated that this system compares favorably over existing coherent modulation techniques. This approach will enable the advantages of massive numbers of RIS passive elements, as well as supporting medium/high mobility and/or low-SNR scenarios. In contrast to coherent demodulation schemes, the presented analysis of the SINR revealed that the non-coherent scheme's performance is not only improved by many BS antennas, but it can be strongly improved by increasing the number of RIS passive elements.

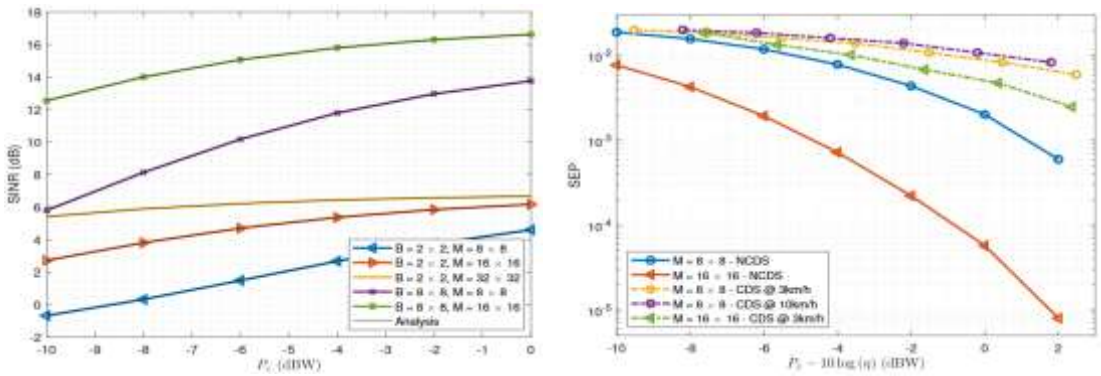

Figure 4-14: **Performance of the proposed non-coherent demodulation scheme. (left) SINR performance Different values of number of antennas (B) and passive elements (M) are considered. (right) Symbol Error Probability (SEP) between the proposed method and the baseline coherent demodulation schemes.**

Perspective and relation to other WP4 contributions

Like the previous contribution, a RIS-modulation architecture is proposed. In the latter case, the considered system concerns a MIMO-OFDM system.

5 Data flow, signalling and time diagrams

In this section, we provide the data flow and signaling, and time diagrams of the RISE-6G architectures for the contributions given in Section □ and Section 4. Here, we show these diagrams for the operation of access, CE, and MEC of RIS-empowered systems, in order to provide examples on how the data and control are exchanged for very different operations. We chose not to present the diagram for every contribution to avoid overwhelming the document. Nevertheless, the data and time diagrams can be easily extended for all the contributions presented.

5.1 UE initial access

Here, we provide an example of data and time flow for the UE initial access discussed in Section 4.2.1. In particular, we provide the data and control flow of Contribution #B-0 (see section 4.4.1) in Figure 5-1, and the corresponding time diagram in Figure 5-2, where the operation of the main actors (i.e., BS, RIS and UEs) are detailed. We mention that *S* is used to represent the number of configuration profiles available at the RIS. The configurations are provided by the BS, hence, the scenario corresponds to the BS-side control. We focus on the access procedure only, without considering the DL feedback for scheduling the user, which is left for future Deliverables.

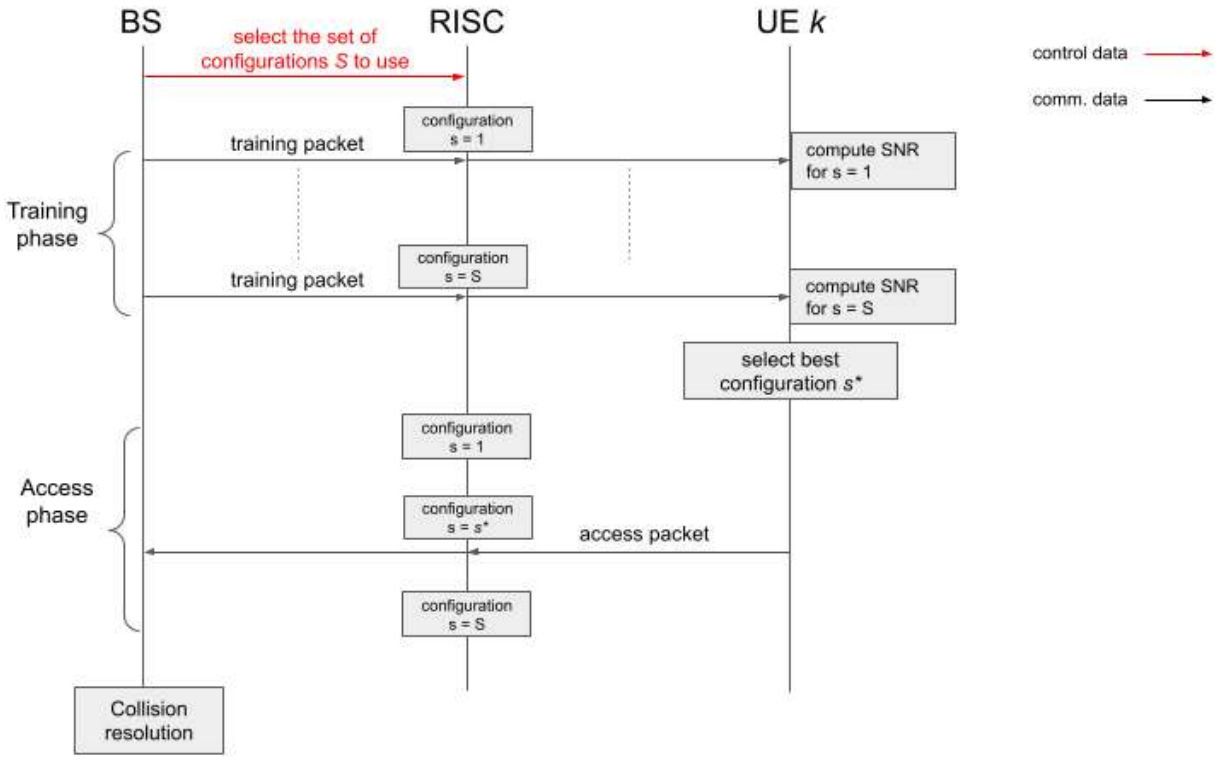

Figure 5-1: Data-flow diagram for UE initial access protocol of contribution #B-0

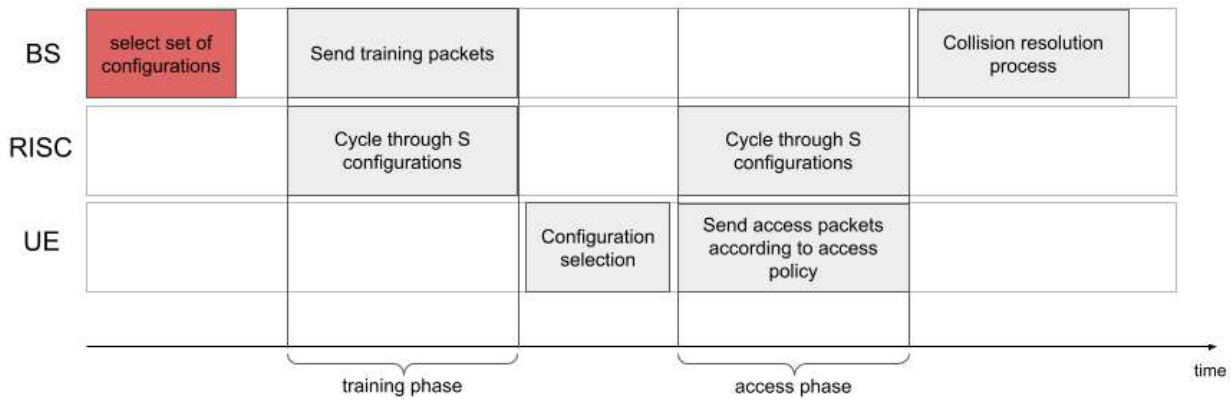

Figure 5-2: Time-flow diagram for UE initial access protocol of contribution #B-0

5.2 Channel estimation process

Here, we provide the data flow of the standard channel estimation process when a RIS is involved. An uplink scenario illustrated in **Errore. L'origine riferimento non è stata trovata.** is performed for the s ake of clarity. The surface changes its configuration at every pilot transmission to allow for the estimation of the cascaded channel. Two control protocols can be applied: In the first case, the RIS is notified that the estimation process starts, and from this point onwards it changes its configuration in a pre-specified manner. This has the benefit of minimal control overhead, but it requires synchronization. In the second protocol, for every pilot exchange, the sending node transmits a control signal to the surface instructing it to change its configuration, and then pilot is transmitted. In this case, the number of control signals is larger, but no synchronization is required, if the receiving end is aware of the order of the selected configurations.

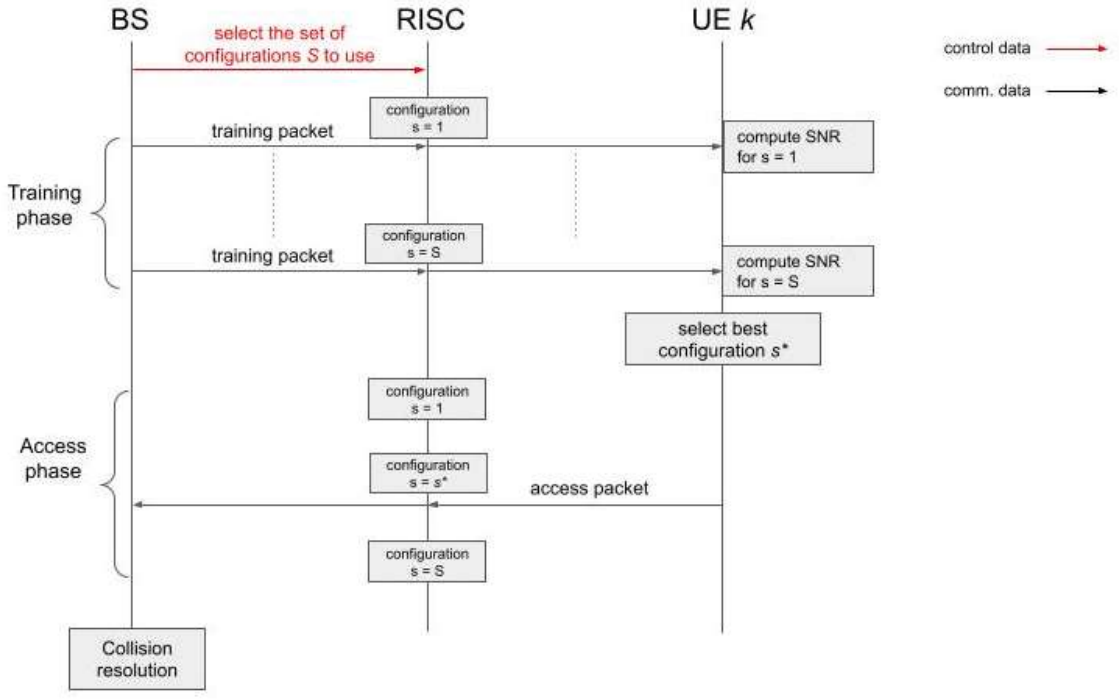

Figure 5-3: Uplink channel estimation process in RIS-empowered environments

5.3 RIS-empowered Mobile Edge Computing

Here, we provide an example of data and time flow for MEC empowered by RISs, which was discussed in Section 3.3.5. The data flow diagram of the methodology is reported in Figure 5-4, where all the required exchange of information among the main actors (i.e., UEs, RIS, AP, and the ES) is detailed. As we can see, there are three separate phases: i) Access, ii) CSI estimation and resource optimisation, iii) computation offloading.

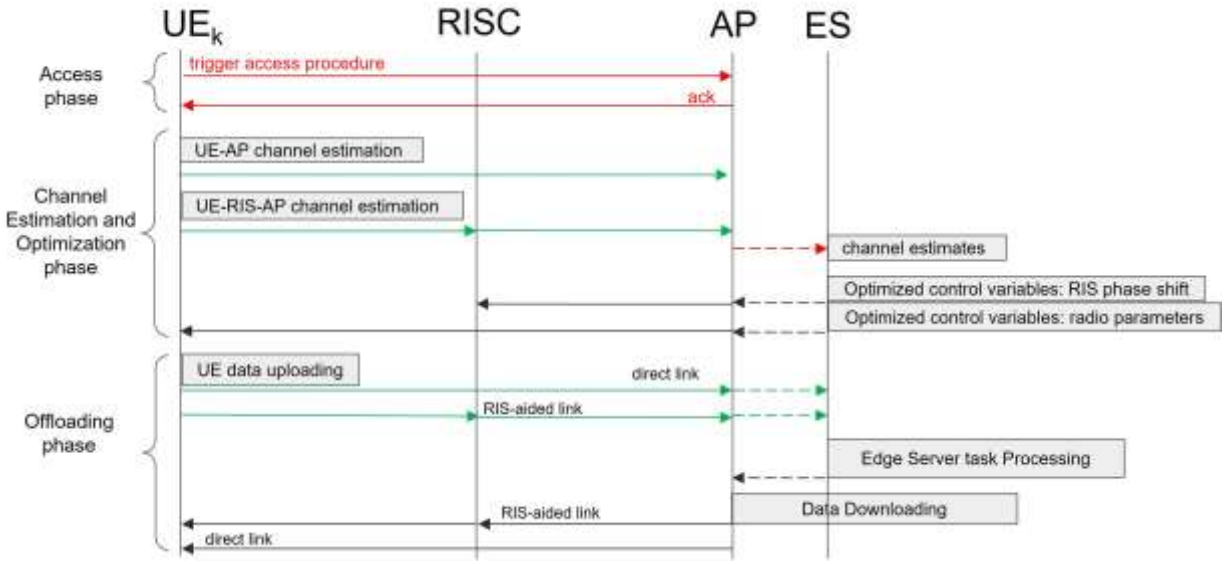

Figure 5-4: Data-flow diagram for RIS-empowered MEC of contribution #A-4

The time flow diagram of the proposed methodology is reported in Figure 5-5, where the sequence of the actions carried out by the main involved actors (i.e., ES, AP, RIS, and UEs) are detailed with respect to the structure of the time slot.

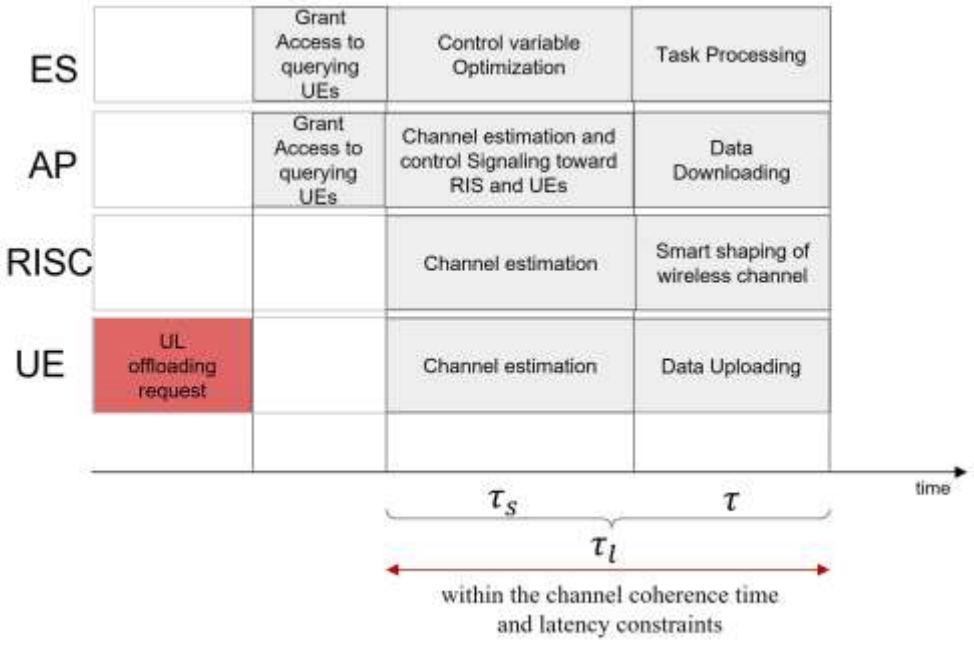

Figure 5-5: Time-flow diagram for RIS-empowered MEC of contribution #A-4

6 Conclusions and outlook

RISs largely extend the capabilities of conventional networks for providing boosted coverage areas in both uplink and downlink, enhancing connectivity and reliability, and enabling edge computing services. From a communication perspective, the basic functionality of the RIS is to enable an alternative path between the BS and the UE to boost specific performance metrics (e.g., rate, latency, etc.), and cope with possible impairments of the direct link due to, e.g., channel blocking events. Then, new architectures must be designed to incorporate multiple RISs into communication networks, with the final aim of boosting connectivity thanks to the possibility of shaping the wireless propagation environment on-demand. A variety of new configurations for RIS-empowered communications are thus possible, and this deliverable has illustrated several important examples. For instance, RISs can be integrated in the wireless networks in a static fashion (e.g., by mounting them on the facade of buildings) or in a nomadic fashion (e.g., by mounting them on moving objects such as UAVs). Also, RIS can be integrated to specifically serve communications and/or edge computing services.

To benefit of the several advantages offered by RISs, a fine control of the RISs as well as novel signalling is clearly needed. RISs can act in a controlled manner, where the BS and the RIS controller act in a coordinated way to jointly optimise the active beamforming at the BS and/or at the receiver-side, and the passive beamforming at the RIS. In such a case, RIS control and signalling can happen via tailored in-band or out-of-band CCs. In-band control channels require a reliable communication between RIS controller and RISs, impacting on the choice of resource allocation and RIS configuration. This constraint is relaxed for the out-of-band channel, leading to a simpler control design. However, the possibility of optimising both control and communication parameters may lead to higher performance.

On the other side, RIS can act in an autonomous manner, when non explicit CC is present. In such a way, the RIS controller optimises the RIS based only on local CSI. This configuration facilitates agile deployment and configuration of the RIS devices, but RIS hardware needs to have the capability to process the incoming signal to acquire local CSI, therefore quasi-active or active hardware configuration is necessary.

The presence of a RIS in a network influences the access procedures, which should take into account the initial access of UEs, and the access to the RIS controller. Typically, the requirement needed for let the RIS work as intended regard sensing and channel estimation, KPI estimation and the algorithmic part (i.e., resource optimisation and configuration of the RIS). A crucial aspect in RIS-empowered communications regard the estimation of the cascade UE-RIS-BS channel, which must be periodically repeated to cope with the variations of the wireless channel. Such operation might be too complex in practical scenarios, and autonomous RIS endowed with learning capabilities can relax such stringent assumption.

In conclusion, it is the recommendation from this deliverable that the RISE-6G architecture should support all the aforementioned alternatives and define the interfaces and signals between the different entities in the architecture (UE, BS, RIS, RISC, ES). At a minimum, the RISE-6G architecture should support: (i) Synchronization among RISs, BSs, and UEs; (ii) Acquisition of the RIS-aided CSI; (iii) a RIS controller that adapts the configuration of the RIS in either a controlled or autonomous fashion.

References

[AA20]	G.T. de Araújo, and A. L. F. de Almeida, “PARAFAC-Based Channel Estimation for Intelligent Reflective Surface Assisted MIMO System,” in Proc. IEE SAM, Hangzhou, China, Jun. 2020, pp. 1-6.
[AAS21]	I. Alamzadeh, G. C. Alexandropoulos, N. Shlezinger, and M. F. Imani, "A reconfigurable intelligent surface with integrated sensing capability," Nature Scientific Reports, vol. 11, no. 20737, pp. 1–10, Oct. 2021.
[AAT16]	V. S. Asadchy, M. Albooyeh, S. N. Tcvetkova, A. Díaz-Rubio, Y. Ra'di, and S. A. Tretyakov, “Perfect control of re-flection and refraction using spatially dispersive metasurfaces,” Phys. Rev. B 94, 075142 – 19 August 2016.
[ACP22]	[ACP22] G. C. Alexandropoulos, M. Crozzoli, D.-T. Phan-Huy, K. D. Katsanos, H. Wymeersch, P. Popovski, P. Ratajczak, Y. Bénédic, M.-H. Hamon, S. Herraiz Gonzalez, R. D'Errico, and E. Calvanese Strinati, "Smart wireless environments enabled by RISs: Deployment scenarios and two key challenges," *Joint European Conference on Networks and Communications & 6G Summit*, Grenoble, France, 7–10 June 2022, pp. 1–6.
[ADS22]	A. Albanese, F. Devoti, V. Sciancalepore, M. Di Renzo, and X. Costa-Ṕerez, “MARISA: A Self-configuring Metasurfaces Absorption and Reflection Solution Towards 6G,” in IEEE INFOCOM 2022 - IEEE Conference on Computer Communications, 2022.
[AES22]	Albanese, A., Encinas-Lago, G., Sciancalepore, V., Costa-Pérez, X., Phan-Huy, D.-T., & Ros, S., "RIS-Aware Indoor Network Planning: The Rennes Railway Station Case," in Proceedings of the IEEE International Conference on Communications (ICC) 2022, [Online] http://arxiv.org/abs/2201.07591
[AJH20]	S. Alfattani, W. Jaafar, Y. Hmamouche, H. Yanikomeroglu, A. Yongac ̧oglu, N. D. Đ`ao, and P. Zhu, “Aerial platforms with reconfigurable smart surfaces for 5G and beyond,” IEEE Communications Magazine, no. January, pp. 96–102, 2020.
[AMD22]	F. Ezzahra Airod, M. Merluzzi, P. Di Lorenzo, and E. Calvanese Strinati, Reconfigurable Intelligent Surface Aided Mobile Edge Computing over Intermittent mmWave Links, proc. of IEEE SPAWC, 2022.
[APV21]	N. Awarkeh, D. -T. Phan-Huy and R. Visoz, "Electro-Magnetic Field (EMF) a-ware beamforming assisted by Reconfigurable Intelligent Surfaces," 2021 IEEE 22nd International Workshop on Signal Processing Advances in Wireless Com-munications (SPAWC), 2021, pp. 541-545.
[APV221]	N. Awarkeh, D.-T. Phan-Huy, R. Visoz, M. di Renzo "A Novel RIS-Aided EMF-Aware Beamforming Using Directional Spreading, Truncation and Boosting," accepted to EuCNC 2022.
[APV222]	N. Awarkeh, D.-T. Phan-Huy, M. di Renzo "A Novel RIS-Aided EMF Exposure Aware Approach Using an Angularly Equalized Virtual Propagation Channel," accepted to EuCNC 2022.
[ASA21]	G. C. Alexandropoulos, N. Shlezinger, I. Alamzadeh, M. F. Imani, H. Zhang, and Y. C. Eldar, "Hybrid reconfigurable intelligent metasurfaces: Enabling simultaneous tunable reflections and sensing for 6G wireless communications," IEEE Communications Magazine, under revision, 2021.
[ASC21]	A. Albanese, V. Sciancalepore, and X. Costa-Perez, “SARDO: An Automated Search-and-Rescue Drone-based Solution for Victims Localisation,” IEEE Transactions on Mobile Computing, pp. 1–12, 2021.

[ASH22]	G. C. Alexandropoulos, K. Stylianopoulos, C. Huang, C. Yuen, M. Bennis, and M. Debbah, "Pervasive machine learning for smart radio environments enabled by reconfigurable intelligent surfaces," IEEE Proceedings, under revision, 2022.
[AV20]	G. C. Alexandropoulos and E. Vlachos, "A hardware architecture for reconfigurable intelligent surfaces with minimal active elements for explicit channel estimation," in Proc. IEEE International Conference on Acoustics, Speech, and Signal Processing, Barcelona, Spain, 4–8 May 2020, pp. 9175–9179.
[BSD14]	S. Barbarossa, S. Sardellitti, and P. Di Lorenzo, "Communicating while computing: Distributed mobile cloud computing over 5G heterogeneous networks," IEEE Signal Proc. Mag., vol. 31, no. 6, pp. 45–55, 2014.
[CAG22]	K. Chen-Hu, G. C. Alexandropoulos, and A. García Armada, "Non-Coherent MIMO-OFDM uplink empowered by the spatial Diversity in reflecting surfaces," IEEE Wireless Communications and Networking Conference, Austin, USA, 10–13 April 2022, to be presented.
[CAS21]	E. Calvanese Strinati, G. C. Alexandropoulos, V. Sciancalepore, M. Di Renzo, H. Wymeersch, D.-T. Phan-Huy, M. Crozzoli, R. D'Errico, E. De Carvalho, P. Popovski, P. Di Lorenzo, L. Bastianelli, M. Belouar, J. E. Mascolo, G. Gradoni, S. Phang, G. Lerosey, and B. Denis, "Wireless environment as a service enabled by reconfigurable intelligent surfaces: The RISE-6G perspective," in *Proc. Joint European Conference on Networks and Communications & 6G Summit*, Porto, Portugal, 8–11 June 2021, pp. 1–6.
[CAW21]	E. Calvanese Strinati, G. C. Alexandropoulos, H. Wymeersch, B. Denis, V. Sciancalepore, R. D'Errico, A. Clemente, D.-T. Phan-Huy, E. De Carvalho, and P. Popovski, "Reconfigurable, intelligent, and sustainable wireless environments for 6G smart connectivity," *IEEE Communications Magazine*, vol. 59, no. 10, pp. 99–105, Oct. 2021.
[CSL22]	V. Croisfelt, F. Saggese, I. Leyva-Mayorga, R. Kotaba, G. Gradoni, P. Popovski, "A Random Access Protocol for RIS-Aided Wireless Communications", submitted to IEEE SPAWC, 2022. Online: https://arxiv.org/abs/2203.03377
[DMC21]	Di Lorenzo, P., Merluzzi, M., Strinati, E. C., and Barbarossa, S., "Dynamic Edge Computing empowered by Reconfigurable Intelligent Surfaces," ArXiv:2112.11269, 2021.
[GRT21]	R. Gupta, D. Reebadiya, S. Tanwar, "6G-enabled Edge Intelligence for Ultra -Reliable Low Latency Applications: Vision and Mission," Computer Standards & Interfaces, vol. 77, pp. 103521, 2021.
[HHA20]	C. Huang, S. Hu, G. C. Alexandropoulos, A. Zappone, C. Yuen, R. Zhang, M. Di Renzo, and M. Debbah, "Holographic MIMO surfaces for 6G wireless networks: Opportunities, challenges, and trends," IEEE Wirel. Commun., vol. 27, no. 5, pp. 118–125, Oct. 2020.
[HJU09]	R. Hunger, M. Joham, and W. Utschick, "On the MSE-duality of the broadcast channel and the multiple access channel," IEEE Trans. Signal Process., vol. 57, no. 2, pp. 698–713, Feb. 2009.
[HYS20]	H. Lu, Y. Zeng, S. Jin and R. Zhang, "Aerial Intelligent Reflecting Surface: Joint Placement and Passive Beamforming Design With 3D Beam Flattening," in IEEE Transactions on Wireless Communications, vol. 20, no. 7, pp. 4128-4143, July 2021
[JAB22]	M. Jian, G. C. Alexandropoulos, E. Basar, C. Huang, R. Liu, Y. Liu, and C. Yuen, "Reconfigurable intelligent surfaces for wireless communications: Overview of hardware designs, channel models, and estimation techniques," TUP and ITU Intelligent and Converged Networks, vol. 3, no.1, pp. 1-32, March 2022.
[JNS21]	V. Jamali, M. Najafi, R. Schober, H. V. Poor, "Power efficiency, overhead, and complexity tradeoff of IRS codebook design—Quadratic phase-shift profile". IEEE Communications Letters, 25(6), 2048-2052.

[LDY20]	S. Li, B. Duo, X. Yuan, Y. C. Liang, and M. DI Renzo, “Reconfigurable Intelligent Surface Assisted UAV Communication: Joint Trajectory Design and Passive Beamforming,” IEEE Wireless Communications Letters, vol. 9, no. 5, pp. 716–720, 2020
[MDB21]	Mattia Merluzzi, Paolo Di Lorenzo, and Sergio Barbarossa, “Wireless edge machine learning: Resource allocation and trade-offs,” IEEE Access, vol. 9, pp. 45377–45398, 2021.
[MDS21]	P. Mursia, F. Devoti, V. Sciancalepore and X. Costa-Pérez, "RISe of Flight: RIS-Empowered UAV Communications for Robust and Reliable Air-to-Ground Networks," in IEEE Open Journal of the Communications Society, vol. 2, pp. 1616-1629, 2021.
[MFC21]	E. Moro, I. Filippini, A. Capone and D. De Donno, "Planning Mm-Wave Access Networks With Reconfigurable Intelligent Surfaces," 2021 IEEE 32nd Annual International Symposium on Personal, Indoor and Mobile Radio Communications (PIMRC), 2021, pp. 1401-1407.
[MSB18]	M. Mozaffari, W. Saad, M. Bennis, Y. H. Nam, and M. Debbah, “A tutorial on UAVs for wireless networks: Applications, challenges, and open problems,” IEEE Communications Surveys and Tutorials, vol. 21, no. 3, pp. 2334–2360, 2018.
[MSG21]	P. Mursia, V. Sciancalepore, A. Garcia-Saavedra, L. Cottatellucci, X. C. Pérez and D. Gesbert, "RISMA: Reconfigurable Intelligent Surfaces Enabling Beamforming for IoT Massive Access," in IEEE Journal on Selected Areas in Communications, vol. 39, no. 4, pp. 1072-1085, April 2021, doi: 10.1109/JSAC.2020.3018829.
[NTH19]	A. Ndikumana, N. H. Tran, T. M. Ho, Z. Han, W. Saad, D. Niyato, and C. S. Hong, “Joint communication, computation, caching, and control in big data multi-access edge computing,” IEEE Transactions on Mobile Computing, pp. 1–1, 2019.
[PHS05]	C B Peel, B M Hochwald, and A L. Swindelhurst, “A Vector-Perturbation Technique for Near-Capacity Multiantenna Multiuser Communication - Part I: Channel Inversion and Regularization,” IEEE Trans. Commun., vol. 53, no. 1, pp. 195–202, Jan. 2005.
[PSZ21]	X. Pang, M. Sheng, N. Zhao, J. Tang, D. Niyato, and K.-K. Wong, “When UAV Meets IRS: Expanding Air-Ground Networks via Passive Reflection,” IEEE Wireless Communications, vol. 28, no. 5, pp. 1–7, 2021.
[SAH22]	K. Stylianopoulos, G. C. Alexandropoulos, C. Huang, C. Yuen, M. Bennis, and M. Debbah, "Deep contextual bandits for orchestrating multi-user MISO systems with multiple RISs," IEEE International Conference on Communications, Seoul, South Korea, 16–20 May 2022, to be presented.
[SDE19]	N. Shlezinger, O. Dicker, Y. C. Eldar, I. Yoo, M. F. Imani, and D. R. Smith, “Dynamic metasurface antennas for uplink massive MIMO systems,” IEEE Trans. Commun., vol. 67, no. 10, pp. 6829–6843, Oct. 2019.
[SSH04]	Q. H. Spencer, A.L. Swindlehurst, and M. Haardt (2004). Zero-forcing methods for downlink spatial multiplexing in multiuser MIMO channels. IEEE Transactions on Signal Processing, 52(2), 461–471.
[SSH22]	K. Stylianopoulos, N. Shlezinger, P. del Hougne, and G. C. Alexandropoulos, "Deep-learning-assisted configuration of reconfigurable intelligent surfaces in dynamic rich-scattering environments," IEEE International Conference on Acoustics, Speech, and Signal Processing, Singapore, 22–27 May 2022, to be presented.
[TKB22]	R. A. Tasci, F. Kilinc, E. Basar, and G. C. Alexandropoulos, “A new RIS architecture with a single power amplifier: Energy efficiency and error performance analysis,” IEEE Access, to appear, 2022.
[WHA21]	L. Wei, C. Huang, G. C. Alexandropoulos, C. Yuen, Z. Zhang, and M. Debbah, "Channel estimation for RIS-empowered multi-user MISO wireless communications," IEEE Transactions on Communications, vol. 69, no. 6, pp. 4144–4157, June 2021.

[WHG22]	L. Wei, C. Huang, Q. Guo, Z. Yang, Z. Zhang, G. C. Alexandropoulos, C. Yuen, and M. Debbah, "Joint channel estimation and signal recovery for RIS-empowered multi-user communications," IEEE Transactions on Communications, under revision.
[XH21]	F. Xin and Y. Huo. “An Overview of Low latency for Wireless Communications: An Evolutionary Perspective,” 2021 Online: https://arxiv.org/abs/2107.03484
[YWL21]	J. Yuan, M. Wen, Q. Li, E. Basar, G. C. Alexandropoulos, and G. Chen, "Receive quadrature reflecting modulation for RIS-empowered wireless communications," IEEE Transactions on Vehicular Technology, vol. 70, no. 5, pp. 5121–5125, May 2021.
[ZSA21]	H. Zhang, N. Shlezinger, I. Alamzadeh, G. C. Alexandropoulos, M. F. Imani, and Y. C. Eldar, "Channel estimation with simultaneous reflecting and sensing reconfigurable intelligent metasurfaces," IEEE International Workshop on Signal Processing Advances in Wireless Communications, Lucca, Italy, 27–30 September 2021, pp. 1–6.